Journal of Biological Systems
Vol. 21, No. 4 (2013) 1340001 (49 pages)

DOI: 10.1142/S0218339013400019

IMPACT OF AGE-DEPENDENT RELAPSE AND IMMUNITY ON MALARIA DYNAMICS

KATIA VOGT-GEISSE*,§, CHRISTINA LORENZO†
and ZHILAN FENG‡

Department of Mathematics, Purdue University
150 N. University Street, West Lafayette
Indiana 47907, USA
**kvogtgei@math.purdue.edu*
†*clorenzo@math.purdue.edu*
‡*zfeng@math.purdue.edu*

Received 10 February 2013
Accepted 7 September 2013
Published 20 January 2014

An age-structured mathematical model for malaria is presented. The model explicitly includes the human and mosquito populations, structured by chronological age of humans. The infected human population is divided into symptomatic infectious, asymptomatic infectious and asymptomatic chronic infected individuals. The original partial differential equation (PDE) model is reduced to an ordinary differential equation (ODE) model with multiple age groups coupled by aging. The basic reproduction number $\mathcal{R}_0$ is derived for the PDE model and the age group model in the case of general n age groups. We assume that infectiousness of chronic infected individuals gets triggered by bites of even susceptible mosquitoes. Our analysis points out that this assumption contributes greatly to the $\mathcal{R}_0$ expression and therefore needs to be further studied and understood. Numerical simulations for $n = 2$ age groups and a sensitivity/uncertainty analysis are presented. Results suggest that it is important not only to consider asymptomatic infectious individuals as a hidden cause for malaria transmission, but also asymptomatic chronic infections (>60%), which often get neglected due to undetectable parasite loads. These individuals represent an important reservoir for future human infectiousness. By considering age-dependent immunity types, the model helps generate insight into effective control measures, by targeting age groups in an optimal way.

Keywords: Malaria; Endemic Model; Age-structure; Reproductive Number; Uncertainty and Sensitivity Analysis.

1. Introduction

Malaria is a vector-borne infectious disease caused by parasites of the genus *Plasmodium*. Malaria is a major international health problem, with an annual estimate of 216 million documented cases and around 1 million deaths.[1] The disease is mostly common in tropical and subtropical regions including much of Sub-Saharan Africa,

*Corresponding author.
§Profesor Asociado a la Facultad de Ingenieria Y ciencias de la Universidad Adolfo Ibañez, Santiago, Chile.

Asia and the Americas. Most vulnerable to severe malaria when exposed to the parasite are people with little or no immunity to the disease, such as young children, pregnant women, or travelers coming from regions with no malaria infections.[1] Malaria is a huge economic burden for many countries, with direct costs estimated to be at least US$12 billion per year worldwide.[1] The most common *Plasmodium* species that cause malaria in humans are: *Plasmodium falciparum*, *Plasmodium vivax*, *Plasmodium malariae*, and *Plasmodium ovale*. *P.falciparum* is responsible for over 1 million deaths annually and 75% of the malaria cases worldwide.[2] The parasite is transmitted to humans by the bites of female *Anopheles* mosquitoes. There are different mosquitoes of the genus *Anopheles* responsible for spreading malaria, which differ on breeding habits, lifespan and human-biting habits, depending on the geographical region and on the species.[3,4] *An. gambiae*, one of the highly anthropophilic species (i.e., feeds almost exclusively on humans) is found in Africa where the malaria burden is highest.[3] About 3.3 billion people live in areas at risk of malaria disease, which is the 5th leading cause of death from infectious diseases worldwide.[1]

Across Sub-Saharan Africa, humans have shown to develop immunity against the malaria parasite. In regions where people are almost continuously exposed to the parasite, different types of immunity have been observed: anti-disease immunity (i.e., gives protection against clinical disease), anti-parasite immunity (i.e., gives protection against mainly the asexual stage of the parasite in the body, which controls parasite density) and transmission-reducing immunity (i.e., reduces the transmission from human to mosquito).[5,6] In regions where malaria is endemic, infected adults rarely experience clinical symptoms, even though they test positive for parasitemia and often carry a high load of malaria parasites in their blood that may be lethal to a malaria-naive person.[5,7] On the other hand, children, especially young children, experience clinical symptoms most of the time when infected with *P.falciparum*.[8,9] The general belief is that an age-dependent anti-parasite and anti-disease immunity can be observed in populations exposed almost continuously to the parasite.[5] Studies have shown that this age-dependent immunity is either due to repetitive exposure (for the human to be able to gain an effective immune response to the parasite) or due to immune responses that depend on host development and maturation, or a combination of both.[10,11] Because of the human host's ability to acquire clinical immunity against the infection, it is important to determine how and to what extent asymptomatic parasite carriers may influence malaria transmission. The methods used to measure parasite presence in the body are often not sensitive enough to detect low parasitemia.[12] This suggests that individuals with low parasitemia represent a parasite reservoir for the subsequent transmission season that could have been underestimated. In most malaria regions in Africa, the endemicity of the disease is stable, which is probably because the infectiousness of the human host is very insensitive to anti-malaria interventions.[13] Therefore, human infectiousness to mosquitoes, especially of asymptomatic carriers, is an important aspect to consider when modeling malaria transmission.

An infected human host is able to infect mosquitoes only when the parasites within the human body have evolved into the sexual stage, i.e., when gametocytes are present in the bloodstream. Thus, to determine the infectiousness of a human host, it is important to consider the duration of gametocytemia and the effect of transmission-reducing immunity, which prevents the parasite from developing inside the mosquito mid-gut and stops the cycle.[6] However, it can be difficult to determine, for asymptomatic carriers, how long gametocytes are present in their bloodstream. Nevertheless, it has been observed that the duration of asymptomatic gametocyte carriage decreases with age.[14] It has also been argued that transmission-reducing immunity is expected to be higher in children, since the anti-parasite immunity prevents adults from developing high gametocytemia, whereas kids develop enough gametocytemia to acquire transmission-reducing immunity.[6] The factors which stimulate gamecytogenesis are not very clearly understood.[5,14] Therefore it is important, for the guidance of future studies, to get some insight on how different hypotheses may affect malaria transmission on creation of gametocytes. It has been suggested that environmental factors may be associated with gametocyte production.[15,16] Seasons in the tropics are based on rainfall and are therefore linked to mosquito bionomics. Mosquitoes can be found throughout the year; and thus, seasonal mosquito activity is referred to increased number of mosquitoes in the rainy season.[16] During the dry season, it is expected that the parasite in the body of asymptomatic carriers would be reduced to a minimum amount, but not disappearing completely, leaving them with a chronic infection which is not enough to infect mosquitoes. Evidence has been provided that mosquito saliva has an impact on the parasite during the chronic asymptomatic stage of infection.[17] It has been hypothesized that in tropical regions, where the seasons are defined by mosquito bionomics, the parasite has evolved to respond to the mosquitoes, specifically to the mosquito bites.[15,16] This hypothesis leads to the belief that reappearance of gametocytemia, and so reappearance of infectious asymptomatic carriers may be triggered by susceptible, not yet infectious, mosquito bites[16] on asymptomatic chronic infected individuals. A similar phenomenon has been demonstrated for other vector-borne parasites.[15] This, together with the assumption that partially immune children develop a better transmission-reducing immunity than adults, as well as the knowledge that most adults do not show clinical symptoms, suggests that it is important to study a model that incorporates several aspects: age-dependent immunity, factors responsible to stimulate gametocytogenesis and not only an asymptomatic class, but divide the asymptomatic population into an asymptomatic infectious class (gametocyte carriers) and an asymptomatic chronic infected class (individuals with low parasitemia).

In the first malaria model developed by Sir Ronald Ross in 1911,[18] Ross captured the basic features of malaria and concluded that malaria can be eradicated if the mosquito population can be reduced below a certain threshold. Since then, with the availability of new data and increased knowledge about the parasites,

many extensions of the Ross model have been developed to better understand the disease dynamics of malaria.[19] More detailed biological and epidemiological factors have been included in these extended models including the effects of human age,[20–22] acquired immunity to malaria,[21,23,24] and genetic and spatial heterogeneity of parasite and host,[25] among others. More careful discussions about the model formulation of transmissions between human hosts and mosquitoes (particularly the dependence on the ratio between the host and the vector) can be found in Chitnis *et al.*[26] It has been shown that the age-structure of human hosts and immunity can play an important role in understanding the disease dynamics and control in regions where malaria is endemic.[7,27,28] Age-structure was included in a partial differential equation model by Anderson and May.[20] It was noticed that this model did not fit well with age-dependent prevalence[29] and it was suggested that host immunity should be considered with age.[19] There are also existing models which include an immunity function (e.g., see Ref. 24) or consider separate immune classes (e.g., see Refs. 30 and 31), but most of these models do not include an age-structure of the human host.

We developed a malaria transmission model that considers age-structure of the human host, factors representing various age-dependent immune responses as well as environmental factors that stimulate parasite development and human infectiousness. The model is formulated in a way that allows us to capture several important malaria features including age-dependent anti-disease, anti-parasite and transmission-reducing immunity, asymptomatic infectious and asymptomatic chronic infected individuals, age-dependent infectivity and susceptibility of humans to mosquitoes, as well as seasonal relapse of asymptomatic chronic infections get triggered when bitten by (even only susceptible) mosquitoes. One of the main objectives of this study is to determine how age-dependent host immunity, asymptomatic chronic infections and parasite adaptation to seasonally-variable mosquito bites may impact malaria dynamics, which to the best of our knowledge has not been simultaneously studied previously using mathematical models. The formulation of our model will also allow us to identify the targeted age group(s) for vaccination and treatment/diagnosis strategies. Currently, there are several malaria vaccines under development. One approach is based on targeting one of the different stages of parasite development in the human body. Those vaccines would either aim to prevent clinical symptoms or aim for reductions of human infections. Another approach is based on reducing the disease transmission of the parasites to the mosquito, resembling the transmission-reducing immunity.[32] Because of the fact that different vaccines generate different immunity involved in the malaria transmission process, it is helpful to study models that can be used to examine how distinct immunity aspects, as well as other factors, contribute to the malaria burden. Our model can also be used to identify the most effective disease control strategies. We demonstrate this by examining the effects of these vaccines and treatment on reducing either the reproduction number $\mathcal{R}_0$ and/or the disease prevalence.

In Sec. 2, we present the age-dependent model, which consists of partial differential equations. Section 3 includes the derivation of the basic reproduction number $\mathcal{R}_0$ with a biological interpretation of its components using biologically relevant quantities. This section also includes a stability analysis of the infection-free steady-state, which is shown to be determined by $\mathcal{R}_0$. In Sec. 4, we derived from the partial differential equation (PDE) model a system of ordinary differential equations (ODEs) with multiple age groups of the human host under the assumption that the model parameters are constant within each age group. The basic reproduction number for this ODE model is also obtained using the next generation matrix approach.[33] Section 5 is devoted to numerical simulations of the ODE system, which illustrate the effect of various biological factors on the disease prevalence and on $\mathcal{R}_0$. A sensitivity and uncertainty analysis is also presented in this section. Finally, in Sec. 6, conclusions and discussions are presented.

2. The PDE Model

To incorporate age-dependent immunity, susceptibility, and infectivity, we consider the age density of individuals in each epidemiological class. Specifically, let $s(t,a)$, $i(t,a)$, $i_A(t,a)$, and $j_A(t,a)$ denote the densities of susceptible, symptomatic infectious, asymptomatic infectious, and asymptomatic chronic infected (non-infectious, parasite carriers with low parasitemia) individuals, respectively, at time t of age a. Let $I_v(t)$ and $S_v(t)$ denote the numbers of susceptible and infectious mosquitoes, respectively, at time t. When modeling malaria transmission dynamics, different functional forms have been used for the transmission rates between humans and mosquitoes. A detailed discussion about various forms and the corresponding assumptions are given in Ref. 26, which makes it more transparent to relate the model parameters to field data. The specific forms of transmission rates used in our model are adopted from those in Ref. 26. The force of infection from infectious mosquitoes to susceptible humans, which is denoted by $\lambda_1(t,a)$, is

$$\lambda_1(t,a) = \beta d(a)\frac{I_v(t)}{N_h(t)}. \tag{2.1}$$

Here, β is the number of bites a mosquito can give per day, $d(a)$ is the probability of host infection per bite, and the total number of humans is

$$N_h(t) = \int_0^\infty n(t,a)da \quad \text{with } n(t,a) = s(t,a) + i(t,a) + i_A(t,a) + j_A(t,a). \tag{2.2}$$

Given a successful bite from an infectious mosquito to a susceptible human host, assume that the probability that it leads to a symptomatic infection is k. Let $\gamma(a)$ denote the rate of recovery of a symptomatic infectious individual of age a. An asymptomatic infectious individual of age a ($i_A(a)$) is assumed to become asymptomatic chronic infected ($j_A(a)$) at rate $\gamma_A(a)$. Assume that asymptomatic infectious and asymptomatic chronic infected individuals do not die from the disease.

As pointed out in the Introduction, there is a possibility for non-infectious j_A individuals to relapse and become asymptomatic infectious (i_A), which can be triggered by susceptible mosquito bites. We assume that this happens during a fraction p of a year when the mosquito number rises due to rainfall. We model this rate of relapse by $\lambda_2(t,a)$ with the following form

$$\lambda_2(t,a) = \beta d_A(a)\frac{S_v(t)}{N_h(t)}, \tag{2.3}$$

where $d_A(a)$ is the probability of relapse per bite. The transmission from infectious humans to susceptible mosquitoes is assumed to be

$$\lambda_v(t) = \beta \int_0^\infty \left[c(a)\frac{i(t,a)}{N_h(t)} + c_A(a)\frac{i_A(t,a)}{N_h(t)}\right] da, \tag{2.4}$$

where $c(a)$ and $c_A(a)$ are the probabilities that a susceptible mosquito becomes infectious per bite from infectious symptomatic and asymptomatic humans, respectively. All variables and parameters are listed in Table 1.

Table 1. Description of variables and parameters used in the PDE model.

Var	Description	Units
$s(t,a)$	age density of susceptible humans	humans
$i(t,a)$	age density of symptomatic infectious humans	humans
$i_A(t,a)$	age density of asymptomatic infectious humans	humans
$j_A(t,a)$	age density of asymptomatic chronic infected humans	humans
$N_h(t)$	total number of humans	humans
$S_v(t)$	♯ of susceptible mosquitoes	mosquitoes
$I_v(t)$	♯ of infectious mosquitoes	mosquitoes
$N_v(t)$	total mosquito population	mosquitoes
$P(a)$	$= \exp[-\int_0^a \mu(\sigma)d\sigma]$, survival probability from death	
$\bar{N}_h$	$= \Lambda \int_0^\infty P(a)da$, ♯ of humans in the limiting case	
$\bar{N}_v$	$= b_v/\mu_v$, ♯ of mosquitoes in the limiting case	
Par	**Description**	**Units**
β	♯ of bites one mosquito can give per day	$\frac{\text{bites}}{\text{mosquito}\cdot\text{day}}$
$d(a)$	% of susceptible humans infected per bite	human/bite
$d_A(a)$	% of human relapses per bite	human/bite
$c(a)$	% of mosquitoes infected per bite on humans in $i(t,a)$	mosquito/bite
$c_A(a)$	% of mosquitoes infected per bite on humans in $i_A(t,a)$	mosquito/bite
$f(a)$	per capita birth rate of humans of age a	day^{-1}
$\mu(a)$	per capita natural mortality of humans of age a	day^{-1}
$\delta(a)$	per capita disease death rate of individuals in $i(t,a)$	day^{-1}
$\gamma(a)$	recovery rate of symptomatic humans of age a	day^{-1}
$\gamma_A(a)$	recovery rate of asymptomatic humans of age a	day^{-1}
b_v	per capita mosquito birth rate	mosquito/day
μ_v	per capita mosquito death rate	day^{-1}
p	% of a year with high mosquito density	dimensionless
k	% of new infections being symptomatic	dimensionless
$\lambda_1(t,a)$	human infection (see (2.1))	day^{-1}
$\lambda_2(t,a)$	human relapse (see (2.3))	day^{-1}
$\lambda_v(t,a)$	mosquito infection (see (2.4))	day^{-1}

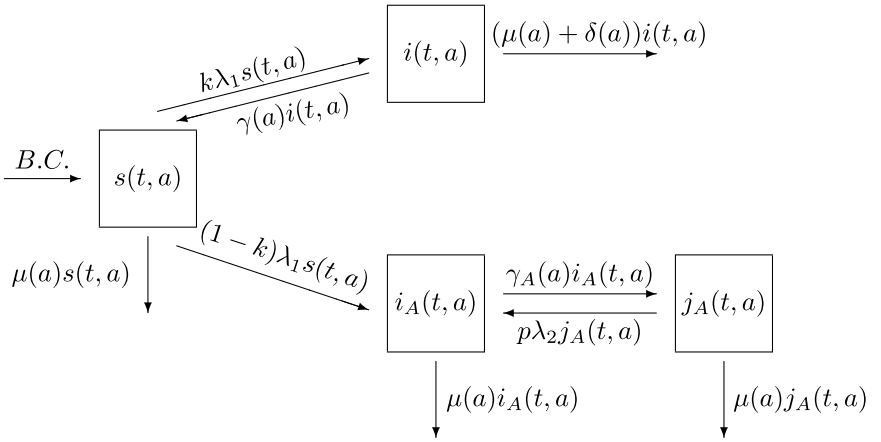

Fig. 1. A diagram for the transitions between epidemiological classes of the human population.

The transitions of humans between the epidemiological classes are depicted in Fig. 1. Following this diagram, we obtain the following equations for humans:

$$\begin{aligned}
\frac{\partial s}{\partial t}+\frac{\partial s}{\partial a} &= -\lambda_1(t,a)s(t,a)-\mu(a)s(t,a)+\gamma(a)i(t,a),\\
\frac{\partial i}{\partial t}+\frac{\partial i}{\partial a} &= k\lambda_1(t,a)s(t,a)-(\gamma(a)+\mu(a)+\delta(a))i(t,a),\\
\frac{\partial i_A}{\partial t}+\frac{\partial i_A}{\partial a} &= (1-k)\lambda_1(t,a)s(t,a)+p\lambda_2(t,a)j_A(t,a)\\
&\quad -(\gamma_A(a)+\mu(a))i_A(t,a),\\
\frac{\partial j_A}{\partial t}+\frac{\partial j_A}{\partial a} &= -p\lambda_2(t,a)j_A(t,a)+\gamma_A(a)i_A(t,a)-\mu(a)j_A(t,a)
\end{aligned} \tag{2.5}$$

with boundary conditions (BC)

$$s(t,0)=\int_0^\infty f(a)n(t,a)da, \quad i(t,0)=0, \quad i_A(t,0)=0, \quad j_A(t,0)=0 \tag{2.6}$$

and initial conditions (IC)

$$s(0,a)=s_0(a), \quad i(0,a)=i_0(a), \quad i_A(0,a)=i_{A0}(a), \quad j_A(0,a)=j_{A0}(a). \tag{2.7}$$

The functions $X_0(a)$ $(X=s,i,i_A,j_A)$ are non-negative with $i_0(a)>0$ for some $a>0$. The forces of infection λ_1, λ_2 and λ_v are given in (2.1), (2.3) and (2.4), respectively. The equations for mosquitoes are

$$\begin{aligned}
\frac{dS_v}{dt} &= b_v-\lambda_v(t)S_v(t)-\mu_v S_v(t),\\
\frac{dI_v}{dt} &= \lambda_v(t)S_v(t)-\mu_v I_v(t)
\end{aligned} \tag{2.8}$$

with ICs $S_v(0) = S_{v0} \geq 0, I_v(0) = I_{v0} \geq 0$. The continuous age-structured model is given by the system of equations in (2.5)–(2.8). It can be shown that the system has a unique non-negative solution for non-negative ICs and that the model is well-posed.

3. Computation of $\mathcal{R}_0$ and Stability of the Disease-Free State for the PDE Model

As in most mathematical models for the spread of infectious diseases, one of the most useful threshold quantities is the basic reproduction number $\mathcal{R}_0$, which usually determines whether the disease can invade into the population (when $\mathcal{R}_0 > 1$) or dies out (when $\mathcal{R}_0 < 1$). The basic reproduction number is defined in general as the average number of secondary infections produced by one infectious individual during the entire infectious period when introduced into a completely susceptible population. In this section, we derive an expression for $\mathcal{R}_0$ by first analyzing the linearized system of (2.5) and (2.8) at the disease-free state, which provides a threshold quantity for the stability condition. By examining the biological interpretation of the threshold quantity, we can confirm that it is indeed the $\mathcal{R}_0$ for the age-structured model.

3.1. *Stable age distribution of the human population in the absence of disease*

Various methods can be used to compute the reproduction number $\mathcal{R}_0$ for age-structured models. We follow the approach of Hadeler and Müller.[34,35] We restrict our attention to the case in which the human population has reached the stable age distribution in the absence of disease. This distribution can be obtained by considering the following equation for the total population $n(t, a) = s(t, a)$,

$$\frac{\partial n}{\partial t} + \frac{\partial n}{\partial a} = -\mu(a)n(t, a) \tag{3.1}$$

with boundary and ICs

$$n(t, 0) = \int_0^\infty f(a)n(t, a)da := B(t), \quad n(0, a) = n_0(a). \tag{3.2}$$

Solving (3.1) and (3.2) along the characteristic lines $a = t + c$ (c is a constant) yields

$$n(t, a) = \begin{cases} n(0, a - t)\mathrm{e}^{-\int_{a-t}^{a} \mu(\sigma)d\sigma}, & \text{if } a \geq t, \\ B(t - a)\mathrm{e}^{-\int_0^a \mu(\sigma)d\sigma}, & \text{if } t > a. \end{cases} \tag{3.3}$$

Substituting (3.3) into (3.2) we have

$$B(t) = \int_0^t f(a)B(t - a)\mathrm{e}^{-\int_0^a \mu(\sigma)d\sigma}da + F_0(t), \tag{3.4}$$

where $F_0(t) = \int_t^\infty f(a)n(0, a - t)\mathrm{e}^{-\int_{a-t}^{a} \mu(\sigma)d\sigma}da \to 0$ as $t \to \infty$.

It can be shown[36] that

$$B(t) = \Lambda e^{\hat{p}t}(1 + \Omega(t)), \tag{3.5}$$

where Λ is a non-negative constant, $\Omega(t)$ is a function with the property $\lim_{t\to\infty} \Omega(t) = 0$, and $\hat{p}$ measures the population growth. Let

$$P(a) = e^{-\int_0^a \mu(\sigma)d\sigma}, \tag{3.6}$$

which represents the probability that an individual survived to age a from natural death. Using (3.3)–(3.6) and considering persistent solutions for large t we obtain the exponential solutions with constant population structure:

$$n(t, a) = \tilde{n}(a)e^{\hat{p}t}, \tag{3.7}$$

where

$$\tilde{n}(a) = \Lambda e^{-\hat{p}a} P(a) \tag{3.8}$$

is the stable age distribution with $\hat{p}$ satisfying the equation

$$\int_0^\infty f(a)P(a)e^{-\hat{p}a}da = 1. \tag{3.9}$$

It is easy to see from (3.7) that if $\hat{p} > 0$ (<0) then the human population will grow (decay) exponentially.

3.2. $\mathcal{R}_0$ and stability of the disease-free equilibrium (DFE)

We determine $\mathcal{R}_0$ by analyzing the stability of the DFE, for which we assume that the total human population has achieved the stable age distribution with constant population size, i.e., $\hat{p} = 0$ and (see (3.7) and (3.8))

$$n(t, a) = \Lambda P(a), \tag{3.10}$$

where $P(a)$ is given in (3.6). In this case, the constraint (3.9) becomes

$$\int_0^\infty f(a)P(a)da = 1. \tag{3.11}$$

For the vector population, notice that $dN_v/dt = b_v - \mu_v N_v$ so that

$$\lim_{t\to\infty} N_v(t) = \frac{b_v}{\mu_v} =: \bar{N}_v. \tag{3.12}$$

By applying the theory of asymptotically autonomous systems,[37] we assume that the vector population has already reached the equilibrium $\bar{N}_v$ in the absence of the disease.

For the remaining analysis in this section, we will consider the limiting system of (2.5) and (2.8) under the conditions

$$n(t, a) = \Lambda P(a), \quad N_h(t) = \Lambda \int_0^\infty P(a)da =: \bar{N}_h, \quad \text{and} \quad N_v(t) = \frac{b_v}{\mu_v} =: \bar{N}_v. \tag{3.13}$$

In this case, the DFE E^* is given by

$$E^* = (s^*, i^*, i_A^*, j_A^*, S_v^*, I_v^*) = (\Lambda P(a), 0, 0, 0, \bar{N}_v, 0). \tag{3.14}$$

To linearize the system, let

$$x(t,a) = s(t,a) - \Lambda P(a) \quad \text{and} \quad X_v(t) = S_v(t) - \bar{N}_v. \tag{3.15}$$

For ease of presentation, introduce the notation

$$\bar{\lambda}_1(a) = \beta d(a)\frac{\Lambda P(a)}{\bar{N}_h}, \quad \bar{\lambda}_2(a) = \beta d_A(a)\frac{\bar{N}_v}{\bar{N}_h}, \quad \text{and} \quad \bar{\lambda}_v = \beta\frac{\bar{N}_v}{\bar{N}_h}, \tag{3.16}$$

where $\bar{N}_h$ and $\bar{N}_v$ are given in (3.13). Then, the linearization of the limiting system is as follows

$$\begin{aligned}
\frac{\partial x}{\partial t} + \frac{\partial x}{\partial a} &= -\bar{\lambda}_1(a)I_v(t) - \mu(a)x(t,a) + \gamma(a)i(t,a),\\
\frac{\partial i}{\partial t} + \frac{\partial i}{\partial a} &= k\bar{\lambda}_1(a)I_v(t) - (\gamma(a) + \mu(a) + \delta(a))i(t,a),\\
\frac{\partial i_A}{\partial t} + \frac{\partial i_A}{\partial a} &= (1-k)\bar{\lambda}_1(a)I_v(t) + p\bar{\lambda}_2(a)j_A(t,a)\\
&\quad - (\gamma_A(a) + \mu(a))i_A(t,a),\\
\frac{\partial j_A}{\partial t} + \frac{\partial j_A}{\partial a} &= -p\bar{\lambda}_2(a)j_A(t,a) + \gamma_A(a)i_A(t,a) - \mu(a)j_A(t,a),\\
\frac{dX_v}{dt} &= -\bar{\lambda}_v\int_0^\infty [c_A(a)i_A(t,a) + c(a)i(t,a)]da - \mu_v X_v(t),\\
\frac{dI_v}{dt} &= \bar{\lambda}_v\int_0^\infty [c_A(a)i_A(t,a) + c(a)i(t,a)]da - \mu_v I_v(t),
\end{aligned} \tag{3.17}$$

where $\bar{\lambda}_1(a)$, $\bar{\lambda}_2(a)$ and $\bar{\lambda}_v$ are given in (3.16).

Consider exponential solutions of the form

$$\begin{aligned}
&x(t,a) = x(a)\mathrm{e}^{\omega t}, \quad i(t,a) = i(a)\mathrm{e}^{\omega t}, \quad i_A(t,a) = i_A(a)\mathrm{e}^{\omega t},\\
&j_A(t,a) = j_A(a)\mathrm{e}^{\omega t}, \quad X_v(t) = \bar{X}_v\mathrm{e}^{\omega t}, \quad \text{and} \quad I_v(t) = \bar{I}_v\mathrm{e}^{\omega t},
\end{aligned} \tag{3.18}$$

where ω is a constant. The stability of E^* can be determined by the sign of ω. Substituting these into equations in (3.17) and canceling $\mathrm{e}^{\omega t}$, we obtain the following equations (it suffices in this case to consider only the $i(a), i_A(a), j_A(a)$ and $\bar{I}_v$ equations):

$$\begin{aligned}
i'(a) &= k\bar{\lambda}_1(a)\bar{I}_v - (\gamma(a) + \mu(a) + \delta(a) + \omega)i(a),\\
i_A'(a) &= (1-k)\bar{\lambda}_1(a)\bar{I}_v + p\bar{\lambda}_2(a)j_A(a) - (\gamma_A(a) + \mu(a) + \omega)i_A(a),\\
j_A'(a) &= \gamma_A(a)i_A(a) - (p\bar{\lambda}_2(a) + \mu(a) + \omega)j_A(a),\\
\omega\bar{I}_v &= \bar{\lambda}_v\int_0^\infty [c_A(a)i_A(a) + c(a)i(a)]da - \mu_v\bar{I}_v.
\end{aligned} \tag{3.19}$$

From the equation for $i(a)$ in (3.19), we obtain:

$$i(a) = \bar{I}_v \int_0^a k\bar{\lambda}_1(\sigma) \mathrm{e}^{-\int_\sigma^a (\gamma(\tau)+\mu(\tau)+\delta(\tau)+\omega)d\tau} d\sigma = \bar{I}_v k F(a,\omega), \tag{3.20}$$

where

$$F(a,\omega) = \int_0^a \bar{\lambda}_1(\sigma) \mathrm{e}^{-\int_\sigma^a (\gamma(\tau)+\mu(\tau)+\delta(\tau)+\omega)d\tau} d\sigma. \tag{3.21}$$

By solving the equation for $i_A(a) + j_A(a)$ in (3.19), i.e.,

$$i_A'(a) + j_A'(a) = (1-k)\bar{\lambda}_1(a)\bar{I}_v - (\mu(a)+\omega)(i_A(a) + j_A(a))$$

we find

$$i_A(a) + j_A(a) = \int_0^a (1-k)\bar{\lambda}_1(\sigma)\bar{I}_v \mathrm{e}^{-\int_\sigma^a (\mu(u)+\omega)du} d\sigma. \tag{3.22}$$

Solving for $j_A(a)$ from (3.22) and substituting it in the $i_A(a)$ equation in (3.19), we obtain

$$\begin{aligned} i_A'(a) = {} & (1-k)\bar{\lambda}_1(a)\bar{I}_v + p\bar{\lambda}_2(a)(1-k)\bar{I}_v \int_0^a \bar{\lambda}_1(\sigma)\mathrm{e}^{-\int_\sigma^a (\mu(\tau)+\omega)d\tau} d\sigma \\ & - (\gamma_A(a) + \mu(a) + p\bar{\lambda}_2(a) + \omega) i_A(a), \end{aligned} \tag{3.23}$$

from which we have

$$i_A(a) = (1-k)\bar{I}_v G(a,\omega,p), \tag{3.24}$$

where

$$G(a,\omega,p) = \int_0^a \left\{ \left[\bar{\lambda}_1(\sigma) + p\bar{\lambda}_2(\sigma) \int_0^\sigma \bar{\lambda}_1(\xi) \mathrm{e}^{-\int_\xi^\sigma (\mu(\tau)+\omega)d\tau} d\xi \right] P_A(a,\sigma,\omega) \right\} d\sigma \tag{3.25}$$

and $P_A(a,\sigma,\omega) := \mathrm{e}^{-\int_\sigma^a (\gamma_A(\tau)+\mu(\tau)+p\bar{\lambda}_2(\tau)+\omega)d\tau}$.

Substituting $i(a)$ and $i_A(a)$ into the $\bar{I}_v$ equation in (3.19) and dividing by $\bar{I}_v$ ($\neq 0$), we obtain the characteristic equation:

$$\begin{aligned} 1 &= \frac{\bar{\lambda}_v}{\omega + \mu_v} \left[\int_0^\infty c_A(a)(1-k)G(a,\omega,p)da + \int_0^\infty c(a)kF(a,\omega)da \right] \\ &=: \Theta(\omega). \end{aligned} \tag{3.26}$$

The function $\Theta(\omega)$ defined in (3.26) can be used to define the basic reproduction number $\mathcal{R}_0$:

$$\mathcal{R}_0 := \Theta(0) = \frac{\bar{\lambda}_v}{\mu_v} \left[\int_0^\infty c_A(a)(1-k)G(a,0,p)da + \int_0^\infty c(a)kF(a,0)da \right], \tag{3.27}$$

where the functions F and G are defined in (3.21) and (3.25), respectively. A biological interpretation of the expression for $\mathcal{R}_0$ defined by (3.27) will be provided at the end of this section. The following result shows that $\mathcal{R}_0 = 1$ provides a threshold condition of the local stability of the DFE E^*.

Theorem 3.1. *The disease-free steady state E^* is locally asymptotically stable if $\mathcal{R}_0 < 1$ and unstable if $\mathcal{R}_0 > 1$.*

The proof of Theorem 3.1 can be found in Appendix A.

3.3. *Interpretation of $\mathcal{R}_0$*

For vector-borne diseases such as malaria, the reproduction number in general includes two components. One is related to human-to-mosquito transmission, which we denote by $\mathcal{R}_{hm}$ and the other is related to mosquito-to-human transmission, which we denote by $\mathcal{R}_{mh}$. As a consequence, the overall reproduction number is (usually) a geometric mean $\sqrt{\mathcal{R}_{hm}\mathcal{R}_{mh}}$. Thus, the expression for $\mathcal{R}_0$ defined in (3.27) is actually $\mathcal{R}_{hm}\mathcal{R}_{mh}$. However, this does not change the threshold condition $\mathcal{R}_0 = 1$ for whether the disease will die out or persist in the population. For notational convenience, we will use the expression of $\mathcal{R}_0$ in (3.27) to describe its biological interpretation, and show that it gives the average number of new infected mosquitoes that one infected mosquito can produce when introduced into a completely susceptible population during its entire infective period.

From (3.16), (3.21), (3.25) and (3.27) we can rewrite $\mathcal{R}_0$ as

$$\begin{aligned}\mathcal{R}_0 = &\int_0^\infty \beta c(a)\left(\frac{1}{\bar{N}_h}\int_0^a k\beta d(\sigma)\frac{P_0(\sigma)}{\bar{N}_h}\frac{1}{\mu_v}\mathrm{e}^{-\int_\sigma^a(\gamma(\tau)+\mu(\tau)+\delta(\tau))d\tau}d\sigma\right)\bar{N}_v da\\ &+\int_0^\infty \beta c_A(a)\left(\frac{1}{\bar{N}_h}\int_0^a (1-k)\beta d(\sigma)\frac{P_0(\sigma)}{\bar{N}_h}\frac{1}{\mu_v}P_A(a,\sigma,0)d\sigma\right)\bar{N}_v da\\ &+\int_0^\infty \beta c_A(a)\left(\frac{1}{\bar{N}_h}\int_0^a p\beta d_A(\sigma)\frac{\bar{N}_v}{\bar{N}_h}\mathcal{J}_A(\sigma)P_A(a,\sigma,0)d\sigma\right)\bar{N}_v da, \qquad (3.28)\end{aligned}$$

where

$$\begin{aligned}\mathcal{J}_A(\sigma) &= \int_0^\sigma (1-k)\beta d(\xi)\frac{P_0(\xi)}{\bar{N}_h}\frac{1}{\mu_v}\mathrm{e}^{-\int_\xi^\sigma \mu(\tau)d\tau}d\xi,\\ P_A(a,\sigma,0) &= \mathrm{e}^{-\int_\sigma^a(\gamma_A(\tau)+\mu(\tau)+p\bar{\lambda}_2(\tau))d\tau}.\end{aligned} \qquad (3.29)$$

The first term in (3.28) represents the contribution from individuals in the $i(a)$ class. The factor

$$k\beta d(\sigma)\frac{P_0(\sigma)}{\bar{N}_h}\frac{1}{\mu_v} \qquad (3.30)$$

is the number of individuals infected at age σ with symptomatic infection by one mosquito during its entire infectious period. The quantity

$$\int_0^a k\beta d(\sigma)\frac{P_0(\sigma)}{\bar{N}_h}\frac{1}{\mu_v}e^{-\int_\sigma^a(\gamma(\tau)+\mu(\tau)+\delta(\tau))d\tau}d\sigma =: \mathcal{I}(a) \tag{3.31}$$

gives the density of symptomatic infectious humans of age $a \in (0,\infty)$ who got infected at age $\sigma < a$ and have not recovered or died at age a. The number of mosquitoes infected by these individuals is

$$\beta c(a)\frac{\mathcal{I}(a)}{\bar{N}_h}\bar{N}_v. \tag{3.32}$$

Thus, the number of mosquitoes infected by symptomatic infectious humans of all age is $\int_0^\infty \beta c(a)\frac{\mathcal{I}(a)}{\bar{N}_h}\bar{N}_v da$, which is the first term in (3.28).

Similarly, the second (third) term in (3.28) represents the contribution from asymptomatic infectious individuals who have not (have) passed through the asymptomatic chronic stage. The quantity

$$\int_0^a (1-k)\beta d(\sigma)\frac{P_0(\sigma)}{\bar{N}_h}\frac{1}{\mu_v}\mathrm{e}^{-\int_\sigma^a(\gamma_A(\tau)+\mu(\tau)+p\bar{\lambda}_2(\tau))d\tau}d\sigma =: \mathcal{I}_{A_1}(a) \tag{3.33}$$

gives the density of asymptomatic infectious humans of age $a \in (0,\infty)$ who were infected at age $\sigma < a$ but have not passed through the asymptomatic chronic stage, and have not recovered or died at age a. Thus, the number of mosquitoes infected by asymptomatic infectious humans of all ages who did not go through the asymptomatic chronic stage is $\int_0^\infty \beta c_A(a)\frac{\mathcal{I}_{A_1}(a)}{\bar{N}_h}\bar{N}_v da$, which is the second term in (3.28). For the third term in (3.28), $\mathcal{J}_A(\sigma)$ is the density of asymptomatic infected humans who were infected at age $\xi < \sigma$ and were still alive and in the asymptomatic infectious-chronic infected-loop at age σ. From these individuals, the number of people who relapse at age σ is

$$p\beta d_A(\sigma)\frac{\bar{N}_v}{\bar{N}_h}\mathcal{J}_A(\sigma). \tag{3.34}$$

The quantity

$$\int_0^a p\beta d_A(\sigma)\frac{\bar{N}_v}{\bar{N}_h}\mathcal{J}_A(\sigma)\mathrm{e}^{-\int_\sigma^a(\gamma_A(\tau)+\mu(\tau)+p\bar{\lambda}_2(\tau))d\tau}d\sigma =: \mathcal{I}_{A_2}(a) \tag{3.35}$$

gives the density of asymptomatic infectious humans who have been through the asymptomatic chronic stage, relapsed at age $\sigma < a$, and have not recovered or died at age a. Thus, the number of mosquitoes infected by asymptomatic infectious humans of all ages who have passed through the asymptomatic chronic stage is $\int_0^\infty \beta c_A(a)\frac{\mathcal{I}_{A_2}(a)}{\bar{N}_h}\bar{N}_v da$, which is the third term in (3.28).

Observe that the third term in (3.28) would not be present in the expression for $\mathcal{R}_0$ if the relapse would occur due to infected mosquitoes ($I_v(t)$) instead of

susceptible mosquitoes ($S_v(t)$). This is because the term $\lambda_2(t,a)j_A(t,a)$ in (2.5) would vanish when linearizing system (2.5) around the DFE.

The $\mathcal{R}_0$ formula (3.28) for the continuous age-structured model can be very helpful for example for evaluating age-dependent vaccination strategies (see, e.g., Refs. 34, 35, 38, 39). For ease of numerical computations, we will derive a system of ODEs from the PDE system by assuming that the human population can be divided into several age groups such that the model parameters within each age group are constant. We will use the ODE system to carry out numerical simulations to examine the influence of various factors on both the reproduction number and the disease prevalence.

4. Reduction of the PDE Model to an ODE System for Discrete Age Groups

Due to the difficulty in analyzing the dependence of disease prevalence to model parameters from the PDE model in Sec. 2, we follow the approach of Hethcote[40] to convert the PDE system to an ODE system. This can be done by dividing the human population into n age groups defined by the n disjoint age intervals, $[a_0, a_1), [a_1, a_2), \ldots, [a_{n-1}, a_n = \infty)$ and assuming that the model parameters in (2.5) are constant in each interval. These age intervals do not need to have equal length. It is important to point out that the ODE system obtained using this approach will include a transition term from one age group to the next due to aging. Although an ODE model that includes these aging terms may increase the difficulty of model analysis more dramatically than multiple age-group models ignoring these terms (which seem to be common), it is necessary to consider the aging factor in order for the ODE system to be comparable to the PDE system.

4.1. *Derivation of the ODE model*

We focus again on the limiting system of the PDE model with the stable age distribution for humans $n(t,a) = n(a) = \Lambda P(a)$, and the constant total population sizes $\bar{N}_h$ and $\bar{N}_v$ for humans and mosquitoes, respectively. Let the constant parameter values in the age interval $a \in [a_{k-1}, a_k)$, $k = 1, \ldots, n$, be denoted by $f(a) = f_k$, $d(a) = d_k$, $d_A(a) = d_{A_k}$, $c(a) = c_k$, $c_A(a) = c_{A_k}$, $\delta(a) = \delta_k$, $\gamma(a) = \gamma_k$, $\gamma_A(a) = \gamma_{A_k}$, and $\mu(a) = \mu_k$. Let

$$N_k(t) = \int_{a_{k-1}}^{a_k} n(t,a)da \tag{4.1}$$

denotes the number of humans in age group k (i.e., ages in $[a_{k-1}, a_k)$) at time t. Then the total number of humans is $\bar{N}_h = \sum_{k=1}^{n} N_k(t)$. Similarly, let $I_k(t), I_{A_k}(t), J_{A_k}(t)$ and $S_k(t)$ denote the number of individuals in age group k in the corresponding

epidemiological classes, i.e.,

$$S_k(t) = \int_{a_{k-1}}^{a_k} s(t,a)da, \quad I_k(t) = \int_{a_{k-1}}^{a_k} i(t,a)da,$$
$$I_{A_k}(t) = \int_{a_{k-1}}^{a_k} i_A(t,a)da, \quad \text{and} \quad J_{A_k}(t) = \int_{a_{k-1}}^{a_k} j_A(t,a)da. \tag{4.2}$$

The force of infection terms in the age interval $[a_{k-1}, a_k)$ $(k = 1, 2, \ldots, n)$ become

$$\lambda_{1k}(t) = \beta d_k \frac{I_v(t)}{N_h(t)}, \quad \lambda_{2k}(t) = \beta d_{A_k} \frac{S_v(t)}{N_h(t)}, \tag{4.3}$$

$$\tilde{\lambda}_v(t) = \beta \sum_{k=1}^{n} \left[c_k \frac{I_k(t)}{N_h(t)} + c_{A_k} \frac{I_{A_k}(t)}{N_h(t)} \right]. \tag{4.4}$$

To derive the ODE for the susceptible humans of age group k we integrate the $s(t,a)$ equation in the limiting PDE system over the age interval $[a_{k-1}, a_k)$, which yields

$$S_k'(t) + s(t,a_k) - s(t,a_{k-1}) = -\lambda_{1k}(t)S_k(t) - \mu_k S_k(t) + \gamma_k I_k(t). \tag{4.5}$$

From Ref. 40, $s(t,a_k) = \alpha_k S_k(t)$ where α_k is the aging rate out of the age group k, which we assume to be time independent and is given by

$$\alpha_k = \frac{n(a_k)}{\int_{a_{k-1}}^{a_k} n(a)da} = \frac{P(a_k)}{\int_{a_{k-1}}^{a_k} P(a)da}, \quad \text{for } k = 1, \ldots, n-1, \tag{4.6}$$

and $\alpha_n = 0$. This rate, α_k, for each age group is the same for all epidemiological classes (i.e., s, i, i_A, j_A), and is a constant, independent of the state variables.

Notice from the constraint (3.11) that

$$\sum_{k=1}^{n} f_k N_k(t) = \sum_{k=1}^{n} f_k \int_{a_{k-1}}^{a_k} n(t,a)da = \int_0^\infty f(a)n(t,a)da$$
$$= \Lambda \int_0^\infty f(a)P(a)da = \Lambda. \tag{4.7}$$

From (4.7), we have

$$s(t,0) = \sum_{k=1}^{n} f_k N_k(t) = \Lambda. \tag{4.8}$$

Replacing $s(t,a_1)$ in (4.5) by $\alpha_1 S_1(t)$ and using (4.8) for $s(t,0)$, we obtain

$$\frac{d}{dt}S_1(t) = \Lambda - \alpha_1 S_1(t) - \lambda_{11}(t)S_1(t) - \mu_k S_1(t) + \gamma_1 I_1(t). \tag{4.9}$$

Similarly, replacing the $s(t,a_k)$ in (4.5) by $\alpha_k S_k(t)$ for $k \geq 2$, we get

$$S_k'(t) = -\lambda_{1k}(t)S_k(t) - \mu_k S_k(t) + \gamma_k I_k(t) - \alpha_k S_k(t) + \alpha_{k-1} S_{k-1}(t). \tag{4.10}$$

We can use the same approach for other equations in system (2.5) and reduce the PDE system in Sec. 2 to the following system of (ODEs)

$$\begin{aligned}
S_1'(t) &= \Lambda - (\alpha_1 + \lambda_{11}(t) + \mu_1)S_1(t) + \gamma_1 I_1(t),\\
I_1'(t) &= k\lambda_{11}(t)S_1(t) - (\gamma_1 + \mu_1 + \delta_1 + \alpha_1)I_1(t),\\
I_{A_1}'(t) &= (1-k)\lambda_{11}(t)S_1(t) + p\lambda_{21}(t)J_{A_1}(t) - (\gamma_{A1} + \mu_1 + \alpha_1)I_{A_1}(t),\\
J_{A_1}'(t) &= -(p\lambda_{21}(t) + \mu_1 + \alpha_1)J_{A_1}(t) + \gamma_{A1}I_{A_1}(t),\\
S_k'(t) &= -(\alpha_k + \lambda_{1k}(t) + \mu_k)S_k(t) + \gamma_k I_k(t) + \alpha_{k-1}S_{k-1}(t),\\
I_k'(t) &= k\lambda_{1k}(t)S_k(t) - (\gamma_k + \mu_k + \delta_k + \alpha_k)I_k(t) + \alpha_{k-1}I_{k-1}(t),\\
I_{A_k}'(t) &= (1-k)\lambda_{1k}(t)S_k(t) + p\lambda_{2k}(t)J_{A_k}(t) - (\gamma_{Ak} + \mu_k + \alpha_k)I_{A_k}(t)\\
&\quad + \alpha_{k-1}I_{A_{k-1}}(t),\\
J_{A_k}'(t) &= -(p\lambda_{2k}(t) + \mu_k + \alpha_k)J_{A_k}(t) + \gamma_{Ak}I_{A_k}(t) + \alpha_{k-1}J_{A_{k-1}}(t),\\
S_v'(t) &= b_v - \tilde{\lambda}_v(t)S_v(t) - \mu_v S_v(t),\\
I_v'(t) &= \tilde{\lambda}_v(t)S_v(t) - \mu_v I_v(t),
\end{aligned} \tag{4.11}$$

for $k = 2, \ldots, n$ with $\alpha_n = 0$.

The ICs for the equations for humans are

$$\begin{aligned}
S_k(0) &= \int_{a_{k-1}}^{a_k} s_0(a)da, \quad I_k(0) = \int_{a_{k-1}}^{a_k} i_0(a)da,\\
I_{A_k}(0) &= \int_{a_{k-1}}^{a_k} i_{A0}(a)da, \quad \text{and} \quad J_{A_k}(0) = \int_{a_{k-1}}^{a_k} j_{A0}(a)da
\end{aligned} \tag{4.12}$$

for $k = 1, \ldots, n$.

4.2. *The basic reproduction number $\mathcal{R}_0$ for the ODE model* (4.11)

Although the formula for $\mathcal{R}_0$ given in (3.28) for continuous age is more convenient to apply in some cases (e.g., age-dependent optimal vaccination problems considered in Refs. 34, 35, 38, 39), the formula of $\mathcal{R}_0$ derived from the ODE system could be much easier to apply in other studies, particularly for numerical computations. We derive a formula of $\mathcal{R}_0$ for discrete age using the next generation matrix approach.[33] The DFE of the system (4.11) is given by

$$\bar{E} = \left(\frac{\Lambda}{\alpha + \mu_1}, \ldots, \frac{\Lambda \prod_{j=1}^{k-1}\alpha_j}{\prod_{j=1}^{k}(\alpha_j + \mu_j)}, \ldots, \frac{\Lambda \prod_{j=1}^{n-1}\alpha_j}{\prod_{j=1}^{n}(\alpha_j + \mu_j)}, 0, \ldots, 0, \bar{N}_v, 0\right). \tag{4.13}$$

Note that the first n components of $\bar{E}$ describe the age distribution of the population at the DFE, i.e.,

$$\bar{N}_k = \frac{\Lambda \prod_{j=1}^{k-1} \alpha_j}{\prod_{j=1}^{k}(\alpha_j + \mu_j)}, \quad k = 1, 2, \ldots, n \ (\alpha_n = 0). \tag{4.14}$$

For ease of notation, let

$$\begin{aligned} &\bar{\gamma}_k = \gamma_k + \mu_k + \delta_k + \alpha_k, \quad \bar{\gamma}_{A_k} = \gamma_{A_k} + \mu_k + \alpha_k, \\ &T_k = \frac{1}{\bar{\gamma}_k}, \quad T_{A_k} = \frac{1}{\bar{\gamma}_{A_k}}, \quad T_v = \frac{1}{\mu_v}, \quad \text{and} \quad \theta_k = \frac{\alpha_k}{\bar{\gamma}_k} \end{aligned} \tag{4.15}$$

for $k = 1, 2, \ldots, n$ with $\alpha_n = 0$. Note that T_k represents the death and aging adjusted mean duration that individuals stay in the I_k stage each time they visit it, T_{A_k} represents the death and aging adjusted mean period of an asymptomatic infected individual during each visit to the I_{A_k} class in age group k, and T_v is the mean infectious period of mosquitoes. The fraction θ_k represents the proportion of symptomatic infectious humans in age group k that survived death and aged to age group $k+1$.

The system (4.11) has $3n + 1$ infected variables, which will be ordered as $(I_1, I_{A_1}, J_{A_1}, \ldots, I_n, I_{A_n}, J_{A_n}, I_v)$. We adopt the notation in Ref. 33 to organize the matrix $\mathcal{F}$ for new infections and the transition matrix $\mathcal{V}$, which are given by

$$\mathcal{F} = \begin{pmatrix} k\lambda_{11}(t)S_1(t) \\ (1-k)\lambda_{11}(t)S_1(t) \\ 0 \\ \vdots \\ k\lambda_{1k}(t)S_k(t) \\ (1-k)\lambda_{1k}(t)S_k(t) \\ 0 \\ \vdots \\ k\lambda_{1n}(t)S_n(t) \\ (1-k)\lambda_{1n}(t)S_n(t) \\ 0 \\ \tilde{\lambda}_v S_v(t) \end{pmatrix}, \quad \mathcal{V} = \begin{pmatrix} \overline{\gamma}_1 I_1(t) \\ -p\lambda_{21}(t)J_{A_1}(t) + \overline{\gamma}_{A_1} I_{A_1}(t) \\ (p\lambda_{21}(t) + \mu_1 + \alpha_1)J_{A_1}(t) - \gamma_{A_1} I_{A_1}(t) \\ \vdots \\ \overline{\gamma}_k I_k(t) - \alpha_{k-1} I_{k-1}(t) \\ -p\lambda_{2k}(t)J_{A_k}(t) + \overline{\gamma}_{Ak} I_{A_k}(t) - \alpha_{k-1} I_{A_{k-1}}(t) \\ (p\lambda_{2k}(t) + \mu_k + \alpha_k)J_{A_k}(t) - \gamma_{A_k} I_{A_k}(t) - \alpha_{k-1} J_{A_{k-1}}(t) \\ \vdots \\ (\gamma_n + \mu_n + \delta_n)I_n(t) - \alpha_{n-1} I_{n-1}(t) \\ -p\lambda_{2n}(t)J_{A_n}(t) + (\gamma_{A_n} + \mu_n)I_{A_n}(t) - \alpha_{n-1} I_{A_{n-1}}(t) \\ (p\lambda_{2n}(t) + \mu_n)J_{A_n}(t) - \gamma_{A_n} I_{A_n}(t) - \alpha_{n-1} J_{A_{n-1}}(t) \\ \mu_v I_v(t) \end{pmatrix}. \tag{4.16}$$

The Jacobian matrices of $\mathcal{F}$ and $\mathcal{V}$ at the DFE are then given by respectively

$$F = \begin{pmatrix} 0 & 0 & \cdots & 0 & 0 & \cdots & 0 & 0 & kh_1 \\ 0 & 0 & \cdots & 0 & 0 & \cdots & 0 & 0 & (1-k)\mathbf{h}_{A_1} \\ & & & & \vdots & & & & \vdots \\ 0 & 0 & \cdots & 0 & 0 & \cdots & 0 & 0 & kh_k \\ 0 & 0 & \cdots & 0 & 0 & \cdots & 0 & 0 & (1-k)\mathbf{h}_{A_k} \\ & & & & \vdots & & & & \vdots \\ 0 & 0 & \cdots & 0 & 0 & \cdots & 0 & 0 & kh_n \\ 0 & 0 & \cdots & 0 & 0 & \cdots & 0 & 0 & (1-k)\mathbf{h}_{A_n} \\ v_1 & \mathbf{v}_{A_1} & \cdots & v_k & \mathbf{v}_{A_k} & \cdots & v_n & \mathbf{v}_{A_n} & 0 \end{pmatrix} \tag{4.17}$$

and

$$V = \begin{pmatrix} \bar{\gamma}_1 & 0 & 0 & 0 & \cdots & 0 & 0 & 0 & 0 & 0 \\ 0 & \mathcal{A}_{A_1} & 0 & 0 & & 0 & 0 & 0 & 0 & 0 \\ -\alpha_1 & 0 & \bar{\gamma}_2 & 0 & \cdots & 0 & 0 & 0 & 0 & 0 \\ 0 & -\mathcal{C}_1 & 0 & \mathcal{A}_{A_2} & \cdots & 0 & 0 & 0 & 0 & 0 \\ & & \vdots & & & & & & & \vdots \\ 0 & 0 & 0 & 0 & \cdots & \bar{\gamma}_{n-1} & 0 & 0 & 0 & 0 \\ 0 & 0 & 0 & 0 & \cdots & 0 & \mathcal{A}_{A_{n-1}} & 0 & 0 & 0 \\ 0 & 0 & 0 & 0 & \cdots & -\alpha_{n-1} & 0 & \bar{\gamma}_n & 0 & 0 \\ 0 & 0 & 0 & 0 & \cdots & 0 & -\mathcal{C}_{n-1} & 0 & \mathcal{A}_{A_n} & 0 \\ 0 & 0 & 0 & 0 & \cdots & 0 & 0 & 0 & 0 & \mu_v \end{pmatrix}. \tag{4.18}$$

Here,

$$\begin{aligned} \mathbf{h}_{A_k} &= \begin{pmatrix} \beta \dfrac{d_k}{\bar{N}_h} \bar{N}_k \\ 0 \end{pmatrix}, \quad h_k = \beta \frac{d_k}{\bar{N}_h} \bar{N}_k, \\ \mathbf{v}_{A_k} &= \left(\beta c_{A_k} \frac{\bar{N}_v}{\bar{N}_h}, 0 \right), \quad v_k = \beta c_k \frac{\bar{N}_v}{\bar{N}_h}, \end{aligned} \tag{4.19}$$

$$\mathcal{C}_k = \begin{pmatrix} \alpha_k & 0 \\ 0 & \alpha_k \end{pmatrix}, \quad \mathcal{A}_{A_k} = \begin{pmatrix} \bar{\gamma}_{A_k} & -p\beta d_{A_k} \dfrac{\bar{N}_v}{\bar{N}_h} \\ -\gamma_{A_k} & p\beta d_{A_k} \dfrac{\bar{N}_v}{\bar{N}_h} + \mu_k + \alpha_k \end{pmatrix}. \tag{4.20}$$

Then the V^{-1} matrix can be written as

$$V^{-1} = \begin{pmatrix} T_1 & 0 & 0 & 0 & \cdots & 0 & 0 & 0 \\ 0 & \mathcal{A}_{A_1}^{-1} & 0 & 0 & \cdots & 0 & 0 & 0 \\ T_2\theta_1 & 0 & T_2 & 0 & \cdots & 0 & 0 & 0 \\ 0 & \mathcal{A}_{A_2}^{-1}\alpha_1\mathcal{A}_{A_1}^{-1} & 0 & \mathcal{A}_{A_2}^{-1} & \cdots & 0 & 0 & 0 \\ \vdots & \vdots & \vdots & \vdots & \vdots & \vdots & \vdots & \vdots \\ T_n\prod_{k=1}^{n-1}\theta_k & 0 & T_n\prod_{k=2}^{n-1}\theta_k & 0 & \cdots & T_n & 0 & 0 \\ 0 & \mathcal{A}_{A_n}^{-1}\prod_{k=1}^{n-1}\alpha_{n-k}\mathcal{A}_{A_{n-k}}^{-1} & 0 & \mathcal{A}_{A_n}^{-1}\prod_{k=1}^{n-2}\alpha_{n-k}\mathcal{A}_{A_{n-k}}^{-1} & \cdots & 0 & \mathcal{A}_{A_n}^{-1} & 0 \\ 0 & 0 & 0 & 0 & \cdots & 0 & 0 & T_v \end{pmatrix} \tag{4.21}$$

and the matrix FV^{-1} is of the following form:

$$FV^{-1} = \begin{pmatrix} 0 & 0 & \cdots & 0 & 0 & kh_1T_v \\ 0 & 0 & \cdots & 0 & 0 & (1-k)\mathbf{h}_{A_1}T_v \\ & & \vdots & & & \vdots \\ 0 & 0 & \cdots & 0 & 0 & kh_kT_v \\ 0 & 0 & \cdots & 0 & 0 & (1-k)\mathbf{h}_{A_k}T_v \\ & & \vdots & & & \vdots \\ 0 & 0 & \cdots & 0 & 0 & kh_nT_v \\ 0 & 0 & \cdots & 0 & 0 & (1-k)\mathbf{h}_{A_n}T_v \\ F_{n,j}\cdot V_{j,1}^{-1} & F_{n,j}\cdot V_{j,2}^{-1} & \cdots & F_{n,j}\cdot V_{j,n-2}^{-1} & F_{n,j}\cdot V_{j,n-1}^{-1} & 0 \end{pmatrix}, \tag{4.22}$$

where

$$F_{n,j}\cdot V_{j,1}^{-1} = v_1T_1 + v_2T_2\alpha_1T_1 + \cdots + v_nT_n\prod_{k=1}^{n-1}\alpha_kT_k, \tag{4.23}$$

$$F_{n,j}\cdot V_{j,2}^{-1} = \mathbf{v}_{A_1}\mathcal{A}_{A_1}^{-1} + \mathbf{v}_{A_2}\mathcal{A}_{A_2}^{-1}\alpha_1\mathcal{A}_{A_1}^{-1} + \cdots + \mathbf{v}_{A_n}\mathcal{A}_{A_n}^{-1}\prod_{k=1}^{n-1}\alpha_{n-k}\mathcal{A}_{A_{n-k}}^{-1}, \tag{4.24}$$

$$F_{n,j}\cdot V_{j,n-2}^{-1} = v_nT_n, \quad F_{n,j}\cdot V_{j,n-1}^{-1} = \mathbf{v}_{A_n}\mathcal{A}_n^{-1}. \tag{4.25}$$

Notice that the matrix FV^{-1} is of rank two and that its trace $\mathrm{tr}(FV^{-1}) = 0$. Therefore, the basic reproduction number $\mathcal{R}_0$, i.e., the dominant eigenvalue of FV^{-1}, is given by

$$\mathcal{R}_0 = \frac{\mathrm{tr}(FV^{-1}) + \sqrt{(\mathrm{tr}(FV^{-1}))^2 - 4E_2(FV^{-1})}}{2} = \sqrt{-E_2(FV^{-1})}, \tag{4.26}$$

where $E_2(FV^{-1})$ is the sum of the principal minors of order two of the matrix FV^{-1}.

4.2.1. *The case of one age group*

To facilitate the biological interpretation of $\mathcal{R}_0$ given by (4.26) we first examine the case of one age group, i.e., $n = 1$. A more detailed description for the matrices F and V can be found in Appendix B.

In this case the matrix FV^{-1} becomes

$$FV^{-1} = \begin{pmatrix} 0 & 0 & 0 & \frac{k\beta d_1}{\bar{N}_h}\bar{N}_1 T_v \\ 0 & 0 & 0 & \frac{(1-k)\beta d_1}{\bar{N}_h}\bar{N}_1 T_v \\ 0 & 0 & 0 & 0 \\ \beta c_1 \frac{\bar{N}_v}{\bar{N}_h} T_1 & \frac{\beta c_{A_1}\frac{\bar{N}_v}{\bar{N}_h}}{\mu_1}\frac{\mu_1 + p\beta d_{A_1}\frac{\bar{N}_v}{\bar{N}_h}}{\bar{\gamma}_{A_1} + p\beta d_{A_1}\frac{\bar{N}_v}{\bar{N}_h}} & \frac{\beta c_{A_1}\frac{\bar{N}_v}{\bar{N}_h}}{\mu_1}\frac{p\beta d_{A_1}\frac{\bar{N}_v}{\bar{N}_h}}{\bar{\gamma}_{A_1} + p\beta d_{A_1}\frac{\bar{N}_v}{\bar{N}_h}} & 0 \end{pmatrix}. \tag{4.27}$$

By applying the formula (4.26) for $n = 1$ (with $\alpha_1 = 0$) we get

$$\begin{aligned} \mathcal{R}_0 &= \sqrt{k\frac{\beta d_1}{\bar{N}_h}\bar{N}_1 T_v \frac{\beta c_1 \bar{N}_v}{\bar{N}_h} T_1 + (1-k)\frac{\beta d_1}{\bar{N}_h}\bar{N}_1 T_v \frac{\beta c_{A_1}\frac{\bar{N}_v}{\bar{N}_h}}{\mu_1}\frac{\mu_1 + p\beta d_{A_1}\frac{\bar{N}_v}{\bar{N}_h}}{\bar{\gamma}_{A_1} + p\beta d_{A_1}\frac{\bar{N}_v}{\bar{N}_h}}} \\ &= \sqrt{kh_1 T_v v_1 T_1 + (1-k)h_1 T_v v_{A_1} T_{h1} P_{I_{A_1}}^{I_{A_1}}}. \end{aligned} \tag{4.28}$$

The biological meaning of the quantities in (4.28) are the following: T_v and T_1 are as in (4.15). $h_1 := \beta\frac{d_1}{\bar{N}_h}\frac{\Lambda}{\mu_1}$ is the number of humans infected by one mosquito per unit of time in a completely susceptible human population; $v_1 := \beta c_1 \frac{\bar{N}_v}{\bar{N}_h}$ is the number of mosquitoes (in a susceptible mosquito population) that one symptomatic infectious human can infect per unit of time; $v_{A_1} := \beta c_{A_1}\frac{\bar{N}_v}{\bar{N}_h}$ is the number of mosquitoes (in a susceptible mosquito population) that one asymptomatic infectious human can infect per unit of time; $T_{h1} := \frac{1}{\mu_1}$ is the lifespan of humans; the quantity $P_{I_{A_1}}^{I_{A_1}}$, given by

$$P_{I_{A_1}}^{I_{A_1}} = \frac{\mu_1 + \rho_1}{\bar{\gamma}_{A_1} + \rho_1}, \quad \text{where } \rho_1 = p\beta d_{A_1}\frac{\bar{N}_v}{\bar{N}_h} \tag{4.29}$$

is the probability that an individual, who entered the $I_{A_1} \leftrightarrows J_{A_1}$ loop through I_{A_1}, is in I_{A_1}. A more detailed explanation for $P_{I_{A_1}}^{I_{A_1}}$ is given in Appendix B.

4.2.2. *The case of $n = 2$ age groups*

For the case of $n = 2$, the matrix FV^{-1} in (4.22) reduces to

$$FV^{-1} = \begin{pmatrix} 0 & 0 & 0 & 0 & kh_1T_v \\ 0 & 0 & 0 & 0 & (1-k)\mathbf{h}_{A_1}T_v \\ 0 & 0 & 0 & 0 & kh_2T_v \\ 0 & 0 & 0 & 0 & (1-k)\mathbf{h}_{A_2}T_v \\ v_1T_1 + v_2\theta_1T_2 & \mathbf{v}_{A_1}\mathcal{A}_{A_1}^{-1} + \mathbf{v}_{A_2}\mathcal{A}_{A_2}^{-1}\alpha_1\mathcal{A}_{A_1}^{-1} & v_2T_2 & \mathbf{v}_{A_2}\mathcal{A}_{A_2}^{-1} & 0 \end{pmatrix}, \tag{4.30}$$

where v_k, $\mathbf{h}_{A_k}$, h_k, $\mathbf{v}_{A_k}$ and $\mathcal{A}_{A_k}$ $(k = 1, 2)$ are given in (4.19) and (4.20) with $\alpha_2 = 0$. Notice that for $k = 1, 2$, $\mathbf{h}_{A_k}$ is a 2×1 vector, $\mathbf{v}_{A_k}$ a 1×2 vector and $\mathcal{A}_{A_k}$ a 2×2 matrix. Hence, the matrix FV^{-1} has dimension seven.

From formula (4.26), the squared reproduction number is

$$\begin{aligned} \mathcal{R}_0^2 = {} & kh_1T_v(v_1T_1 + \theta_1v_2T_2) + kh_2T_vv_2T_2 + (1-k)h_2T_vv_{A_2}P_{I_{A_2}}^{I_{A_2}}T_{h2} \\ & + (1-k)h_1T_v(v_{A_1}T_{h1}P_{I_{A_1}}^{I_{A_1}} + v_{A_2}P_{I_{A_1}}^{I_{A_1}}\theta_{h1}P_{I_{A_2}}^{I_{A_2}}T_{h2} \\ & + v_{A_2}P_{I_{A_1}}^{J_{A_1}}\theta_{h1}P_{J_{A_2}}^{I_{A_2}}T_{h2}). \end{aligned} \tag{4.31}$$

Here, the notation (e.g., h_k, v_k, $P_{I_{A_1}}^{I_{A_1}}$) have similar meanings as in the case of $n = 1$ except the difference due to aging ($\alpha_1 > 0$, $\alpha_2 = 0$). For example, $h_1 = \beta\frac{d_1}{\bar{N}_h}\bar{N}_1$ and $h_2 = \beta\frac{d_2}{\bar{N}_h}\bar{N}_2$ are the numbers of humans infected by one mosquito per unit of time in the completely susceptible human populations in groups one and two, respectively. $v_k = \beta c_k\frac{\bar{N}_v}{\bar{N}_h}$ is the number of mosquitoes (in a susceptible mosquito population) that one symptomatic infectious human can infect per unit of time $(k = 1, 2)$; $v_{A_k} = \beta c_{A_k}\frac{\bar{N}_v}{\bar{N}_h}$ is the number of mosquitoes (in a susceptible mosquito population) that one asymptomatic infectious human can infect per unit of time $(k = 1, 2)$; $T_{h1} = \frac{1}{\alpha_1+\mu_1}$ and $T_{h2} = \frac{1}{\mu_2}$ are the average stage durations of individuals in age groups 1 and 2, respectively; and $\theta_{h1} = \frac{\alpha_1}{\alpha_1+\mu_1}$ represents the disease independent probability that an individual of age group 1 ages to age group 2. T_v, T_1 and T_2 are as in (4.15).

The quantity $P_{I_{A_k}}^{I_{A_k}}$, given by

$$P_{I_{A_k}}^{I_{A_k}} = \frac{\rho_k + \mu_k + \alpha_k}{\bar{\gamma}_{A_k} + \rho_k}, \quad \text{where } \rho_k = p\beta d_{A_k}\frac{\bar{N}_v}{\bar{N}_h}, \quad k = 1, 2, \tag{4.32}$$

represents the probability that an individual, who entered the $I_{A_k} \leftrightarrows J_{A_k}$ loop through I_{A_k}, is in I_{A_k}. Similarly, the quantity

$$P_{I_{A_1}}^{J_{A_1}} = \frac{\gamma_{A_1}}{\bar{\gamma}_{A_1} + \rho_1} \tag{4.33}$$

represents the probability that an individual that entered the $I_{A_1} \leftrightarrows J_{A_1}$ loop through I_{A_1}, is in J_{A_1}; and

$$P_{J_{A_2}}^{I_{A_2}} = \frac{\rho_2}{\rho_2 + \bar{\gamma}_{A_2}} \tag{4.34}$$

represents the probability that an individual, who entered the $I_{A_2} \leftrightarrows J_{A_2}$ loop through J_{A_2}, is in I_{A_2}. A more detailed explanation on the derivation of these quantities can be found in Appendix B.

Therefore, (4.31) represents the secondary number of infected mosquitoes generated by an infectious mosquito via humans in different age groups and different stages. Specifically, the first term corresponds to the contribution from symptomatic infectious individuals who were initially infected in age group 1 (a fraction θ_1 aged to group two). The second term corresponds to the contribution from asymptomatic individuals who were initially infected in age group 1. These individuals enter the $I_{A_1} \leftrightarrows J_{A_1}$ loop through I_{A_1} and then they undergo one of the following three scenarios at a given time: (i) they have not aged and are currently in I_{A_1} where they can infect mosquitoes (see the term $v_{A_1} T_{h1} P_{I_{A_1}}^{I_{A_1}}$ in (4.31)); (ii) they aged while in I_{A_1} (so they entered the $I_{A_2} \leftrightarrows J_{A_2}$ loop through I_{A_2}) and are currently in I_{A_2} (see term $v_{A_2} P_{I_{A_1}}^{I_{A_1}} \theta_{h1} P_{I_{A_2}}^{I_{A_2}} T_{h2}$ in (4.31)); and (iii) they aged while in J_{A_1} (so they entered the $I_{A_2} \leftrightarrows J_{A_2}$ loop through J_{A_2}) and are currently in I_{A_2} (see term $v_{A_2} P_{I_{A_1}}^{J_{A_1}} \theta_{h1} P_{J_{A_2}}^{I_{A_2}} T_{h2}$ in (4.31)).

The third term in (4.31) corresponds to the contribution from symptomatic infectious individuals who were initially infected in age group 2; and the fourth term corresponds to the contribution from asymptomatic individuals who were initially infected in age group 2.

Notice that, as we have already mentioned for the PDE $\mathcal{R}_0$, various terms in the expression for $\mathcal{R}_0$, (4.31), that involve looping would not have appeared without the assumption of relapse triggered by susceptible mosquito bites and instead by infectious mosquito bites.

It is possible to rewrite the expression for $\mathcal{R}_0$ in (4.31) as a linear combination of reproduction numbers of a children population only and an adult population only, in the following way:

$$\mathcal{R}_0^2 = \mathcal{R}_{01}^2 + \mathcal{R}_{02}^2 + \frac{h_1\theta_1}{h_2}\mathcal{R}_{02}^2 \quad \left(= \mathcal{R}_{01}^2 + \mathcal{R}_{02}^2 + \frac{v_2}{v_1}\frac{T_2}{T_1}\theta_1 \mathcal{R}_{01}^2 \right) \quad \text{for } k = 1, \tag{4.35}$$

and

$$\mathcal{R}_0^2 = \mathcal{R}_{01}^2 + \mathcal{R}_{02}^2 + \frac{h_1\theta_1}{h_2}\mathcal{R}_{02S}^2 + \frac{h_1\theta_{h1}}{h_2} P_{I_{A_1}}^{I_{A_1}} \mathcal{R}_{02A}^2 + \frac{h_1\theta_{h1}}{h_2} \frac{P_{I_{A_1}}^{J_{A_1}} P_{J_{A_2}}^{I_{A_2}}}{P_{I_{A_2}}^{I_{A_2}}} \mathcal{R}_{02A}^2 \quad \text{for } k > 1, \tag{4.36}$$

where

$$\mathcal{R}_{01}^2 = \underbrace{kh_1T_vv_1T_1}_{=:\mathcal{R}_{01S}^2} + \underbrace{(1-k)h_1T_vv_{A_1}T_{h_1}P_{I_{A_1}}^{I_{A_1}}}_{=:\mathcal{R}_{01A}^2} \tag{4.37}$$

and

$$\mathcal{R}_{02}^2 = \underbrace{kh_2T_vv_2T_2}_{=:\mathcal{R}_{02S}^2} + \underbrace{(1-k)h_2T_vv_{A_2}T_{h_2}P_{I_{A_2}}^{I_{A_2}}}_{=:\mathcal{R}_{02A}^2} \tag{4.38}$$

are the reproduction numbers for a children only and adult only population (no aging involved) respectively, with their symptomatic ($\mathcal{R}_{01S}^2$, $\mathcal{R}_{02S}^2$) and asymptomatic ($\mathcal{R}_{01A}^2$, $\mathcal{R}_{02A}^2$) contributions. For example in the case $k = 1$ (in which case our model reduces to an SIS model), the term $\frac{h_1\theta_1}{h_2}$ in (4.35), represents the ratio of newly infected children who age into adulthood and newly infected adults. This demonstrates that when aging from one group to the other is involved, the basic reproduction number is not solely a sum of contributions of each age group, but has also extra terms that arise from the equations being coupled by aging.

5. Numerical Simulations and Results

To illustrate how the disease dynamics in different groups may be influenced by various factors represented by the model parameters, we carried out an extensive number of numerical simulations of the ODE system in the case of two age groups. Since the simulation results depend on the choice of parameter values, we performed uncertainty and sensitivity analyses using the Latin Hypercube Sampling approach. These analyses are conducted for both the reproduction number $\mathcal{R}_0$ and the disease prevalence.

5.1. *Parameter values and calibration of the model*

We developed a computer code using the R computer Language and Environment[41] for the ODE system (4.11) for two age groups: children from 0 to 15 years and adults from 16 years on. Although we do not have an analytical result for the existence and stability of endemic equilibrium points, our large number of simulations of the system suggest that when $\mathcal{R}_0 > 1$ there is a unique stable endemic equilibrium. We run the simulations until the endemic equilibrium has been reached (which is 25 years for the parameter values we used). We calibrated the mosquito demographics such that the mosquito population remains constant in time, and calibrated the human birth and death rates such that the population size and age distribution in the absence of disease remain the same. Based on the demographic data reported in Ref. 42, the initial population age distribution is chosen to be 45% children and 55% adults, which will be used for the fractions $\bar{N}_1/\bar{N}_h = 0.45$ and $\bar{N}_2/\bar{N}_h = 0.55$, respectively. For a given population, assume that the total population $\bar{N}_h$ is known.

Notice that, when using the DFE $\bar{N}_1 = \Lambda/(\mu_1 + \alpha_1)$, fixing $\mu_1 = 0.0002$ (day^{-1}) and assuming the aging rate in group one to be $\alpha_1 = 1/(15 \cdot 365)$ per day, we obtain the value of Λ from $\Lambda = \bar{N}_1(\mu_1 + \alpha_1)$. Using $\bar{N}_2 = \frac{\Lambda}{\mu_2}\frac{\alpha_1}{\alpha_1+\mu_1} = 0.55\bar{N}_h$ we get an estimate for $\mu_2 = \alpha_1\frac{\bar{N}_1}{\bar{N}_2} \approx 0.00015$.

Some of the model parameters have been commonly used in previous modeling studies on malaria and can be adopted for our model. For the remaining parameters, particularly the ones that are specific to our model, values are determined so that the simulation results are consistent with available data related to malaria prevalence. For example, the reduction of the population (at the endemic equilibrium) due to disease death is on average 0.25%,[3,8] which our model also produces. We define symptomatic (asymptomatic infectious) prevalence in age group k ($k = 1, 2$) as the fraction of symptomatic (asymptomatic) infectious individuals at the equilibrium, i.e., $I_k/\bar{N}_h$ ($I_{A_k}/\bar{N}_h$). Our results show a symptomatic prevalence of children of approximately 3.2% (see Fig. 2(a)). This is concordant with collected observations in countries of Sub-Saharan Africa like Tanzania, that regions where seasons are often characterized by mosquito bionomics,[43,44] children's prevalence ranges between approximately 2.5% and 15%.[43,45] Out of the symptomatic cases, the majority correspond to children,[46] as can be also seen in Fig. 2(a) of Sec. 5.2.1.

The parameter k represents the proportion of susceptible individuals who become symptomatic upon infection, and depends on innate resistance of individuals. For example, genetically determined traits are selected over generations and contribute to the innate protection against the risk of clinical illness.[47–50] In this study, we assume k to be a constant, although it would be of interest for future work to consider k to be age-dependent if significant evidence for it can be found in the literature, and of which we do not have sufficient knowledge.

In a stable perennial transmission region, the mosquito population starts to grow with the onset of the rainy season and relapse of asymptomatic chronic infected individuals gets triggered by non-infectious mosquito bites.[16] The value 0.4 given to p represents a rainy season of at least 4.8 months.

As for the two age groups we assume for the parameters representing human susceptibility of becoming infectious, that $d_2 < d_1$ due to anti-parasite immunity acquired by adults,[5] even after a few malaria attacks.[51] Because of the higher anti-parasite immunity of adults, we also assume $d_{A_2} < d_{A_1}$. It can be argued, that asymptomatic adults have less asexual parasites in their blood as compared to asymptomatic children, and are therefore less likely to create gametocytes.

For the parameters representing human infectiousness, we assume $c_2 < c_1$ due to a fast gain of transmission-reducing immunity for susceptible humans, as observed for malaria-naive individuals, and in general a higher gametocyte density observed in children.[6,52] Also, a higher anti-parasite immunity in asymptomatic adults produces a lower gametocyte prevalence for these individuals compared to children. Since the presence of gametocytes in the blood is necessary to acquire transmission-reducing immunity, this could imply a lower transmission-reducing immunity in

adults than children,[6] which is why we made the assumption $c_{A_1} < c_{A_2}$, as other studies also suggest.[53] We chose $c_2 < c_{A_2}$ since it has been observed that clinical symptoms stimulate gametocytogenesis[54] and therefore symptomatic adults could develop a better transmission-reducing immunity than asymptomatic individuals. Also, studies have observed that infectiousness of asymptomatic carriers is higher than symptomatic, once gametocytes are present in the blood.[55] Unlike for adults, we assume for children $c_{A_1} < c_1$, since children are longer exposed to gametocytes because of the assumed higher probability of relapse ($d_{A_2} < d_{A_1}$) and the observation that they can show a high density parasitemia without showing symptoms.[54,56,57] Therefore, higher gametocyte densities in children induce higher levels of transmission-reducing activity,[53] which we assume that asymptomatic children keep developing, unlike adults that we assume lose it due to increasing anti-asexual parasite immunity.[52]

Complications due to malaria are worse in children, and their recovery rate is lower than for adults, which is why we chose $\delta_2 < \delta_1$ and $\gamma_1 < \gamma_2$. We assumed a lower duration in the asymptomatic infectious stage for both age groups compared to the time spent in the symptomatic class, as well as a decreasing amount of time spent in the asymptomatic infectious class with age ($\gamma_{A_1} < \gamma_{A_2}$).[56,57]

The aging rate from one age group to the other is represented by the parameter α_1 and is chosen to be 1/15/365 assuming that each age is evenly distributed in the children's age group, such that a fraction of 1/15 individuals move each year from age group 1 to age group 2.

We used the parameters that satisfy our assumptions as base line values for our simulations. Because of the uncertainty of some of the assumptions (due to the difficulties in field studies), in Sec. 5.2.2 we chose a reasonable range for each of the parameters to check robustness of our results. More details on the parameter values and their references can be found in Table 2.

5.2. *Simulation results and interpretations*

We conducted numerical simulations under two scenarios. In the first scenario we used a fixed set of parameter values, and in the second scenario the parameters are allowed to take on values from a set of given regions with a fixed distribution such that the previously fixed value would be the most probable one. In the case of variable parameter values, 1,000 simulations were run with parameter values chosen randomly out of their respective ranges. These simulations can be used to demonstrate the sensitivity of model outcomes to the uncertainty of parameter choices.

5.2.1. *Simulations and results with fixed parameter values*

For the case of fixed parameter values, the choice of parameters leads to the reproduction number $\mathcal{R}_0 = 3.4$. We are mostly interested in the fraction of

Table 2. Parameter values and ranges used in the numerical simulations as well as in the uncertainty and sensitivity analyses.

Parameters	Two age groups		References
Fixed values			
b_v	150		Calibrated
μ_v	0.03		58, 59
Λ	$0.45\bar{N}_h(\mu_1+\alpha_1)$		Calibrated
Values with ranges			
β	0.2 T (0.1, 0.25)		58, 60
k	0.8 U (0.5, 0.9)		
p	0.4 T (0.1, 0.5)		16
Age-dependent	Age group 1	Age group 2	
μ_k	0.0002	$\alpha_1\bar{N}_1/\bar{N}_2$	42
α_k	1/15/365	0	42
δ_k	0.00002 T (0.000001, 0.0001)	0.000002 T (0, 0.0003)	60
d_k	0.03 T (0.01, 0.08)	0.015 T (0.005, 0.08)	60
d_{A_k}	0.02 T (0.005, 0.06)	0.009 T (0.006, 0.015)	16
c_k	0.3 T (0.05, 0.4)	0.24 T (0.12, 0.4)	60
c_{A_k}	0.12 T (0.005, 0.15)	0.4 T (0.01, 0.8)	53, 60
γ_k	1/100 T (1/105, 1/80)	1/80 T (1/90, 1/70)	60
γ_{A_k}	1/65 T (1/100, 1/30)	1/50 T (1/80, 1/30)	14, 56

symptomatic (I), asymptomatic infectious (I_A), and asymptomatic chronic infected (J_A) individuals, as well as the fractions of individuals for each age group (group 1 for children and group 2 for adults) of these classes and their relative densities. Figures 2(a)–2(c) illustrate the fractions of human populations in each of the infected classes within each age group. We observe that for this set of parameter values the endemic equilibrium has been reached after 25 years. Figures 2(a) and 2(b) show that the asymptomatic infectious individuals contribute 2–3 times more than symptomatic infectious individuals. In particular, the fraction of asymptomatic infectious individuals (gametocyte carriers), which are the asymptomatic individuals with parasites in their blood capable of infecting mosquitoes, can be observed in Fig. 2(b). There, we can see a combined age group prevalence of 16% and a decrease in prevalence with age, which has also been observed in previous studies.[14] Detection of low *P.falciparum* parasitemia is a great challenge. Methods

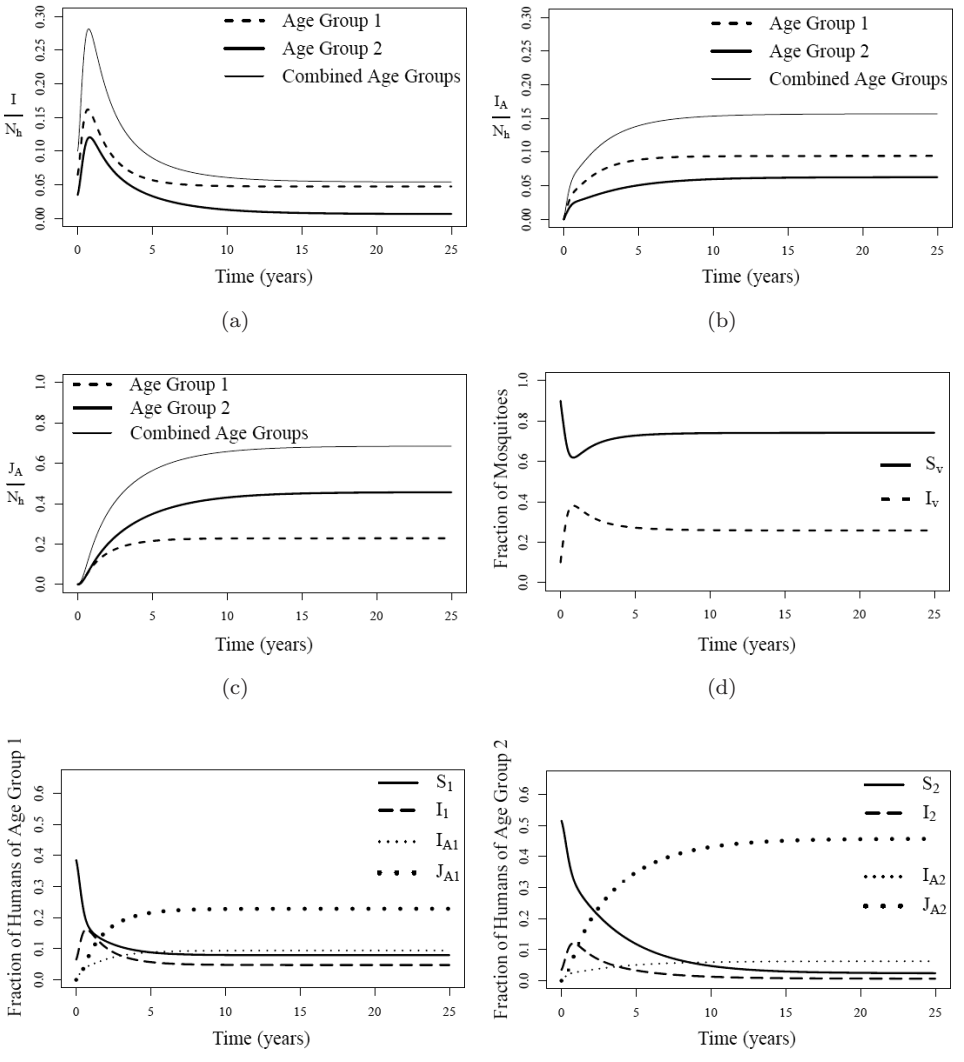

Fig. 2. Numerical simulations of the ODE model with two age groups using fixed parameter values given in Table 2. These parameter values produce an $\mathcal{R}_0$ of 3.4. Plots in (a)–(c) show the fractions of symptomatic infectious individuals, asymptomatic infectious individuals, and asymptomatic chronic infected individuals, respectively, for the two age groups. The plot in (d) is for the mosquito population. Plots in (e) and (f) show all four epidemiological classes for groups 1 and 2, respectively.

like the classic thick blood smear method or rapid diagnostic tests (RDTs) often show decreased sensitivity at lower parasitemia. It has been demonstrated that up to an overall asymptomatic adult prevalence of 52% can be detected by more sensitive tests,[12] a result that our model confirms (see Fig. 3(d)) for $\mathcal{R}_0 > 2$. Studies have

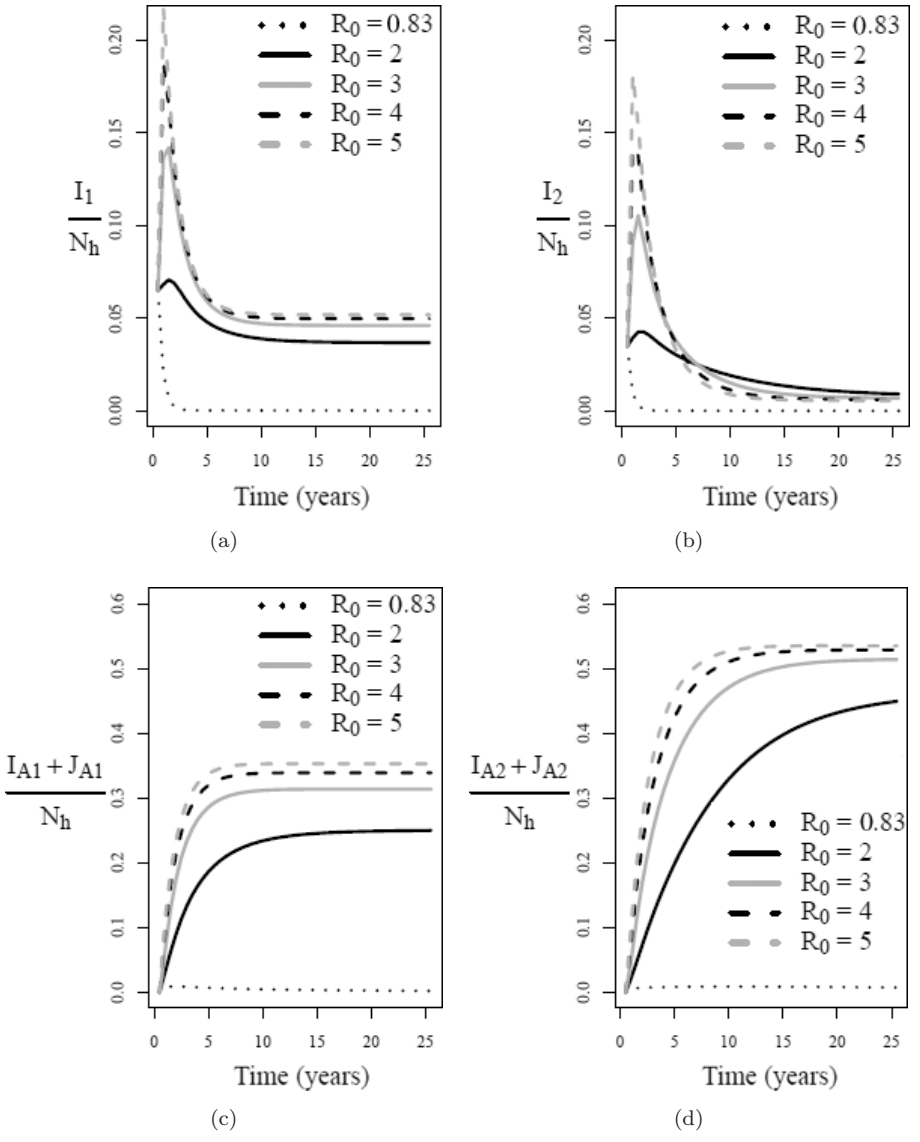

Fig. 3. Numerical simulations of the ODE model with two age groups for different $\mathcal{R}_0$ values, obtained from varying β. For the other parameters the values in Table 2 were used. Plots (a) and (b) show the fractions of symptomatic infectious individuals for age groups 1 and 2 respectively, while (c) and (d) illustrate overall asymptomatic (asymptomatic infectious and asymptomatic chronic infected) individuals for the two age groups.

also estimated, that in some malaria endemic settings 90% of the exposed individuals are likely infected with asymptomatic malaria.[61] For that, our model gives an estimate of approximately 80% (Figs. 3(c) and 3(d)) when combining overall asymptomatic children and adult populations. This value is close to what can be found in

the literature and represents individuals with sexual and asexual parasites in their blood. Figures 3(c) and 3(d) also show that the proportion of overall asymptomatic infection is higher among adults than among children, as can be expected for a malaria endemic area.[5,7] Because of the difficulty of detecting low parasitemia it is important to develop mathematical models that can give information about individuals with low parasitemia. In our model, we call these individuals asymptomatic chronic parasite carriers (J_A), who serve as a reservoir for malaria parasites before the parasites in their body develop into gametocytes.

Our simulations show that the majority of symptomatic infectious (I) and asymptomatic infectious (I_A) individuals are children (see Figs. 2(a) and 2(b)), which is consistent with observed patterns of malaria prevalence and the higher expected gametocyte densities in children.[6,46,52] Nevertheless it is of great importance to notice that over 60% of the population is asymptomatic chronic infected, with twice as many adults than children (see Fig. 2(c)). Adults in this class could be responsible for the persistence of malaria in many regions of Sub-Saharan Africa and need to be taken into consideration. They possibly undergo a relapse of human infectiousness and contribute to the infectious pool for mosquitoes. This indicates that the number of infected cases might be underestimated in field studies due to commonly undetectable parasite loads.

The fractions of infectious and susceptible mosquitoes are plotted in Fig. 2(d). For ease of comparison, Figs. 2(e) and 2(f) show the plots of relative magnitudes of different infected classes within each age group and between age groups. In these plots, we observe a similar trend among age groups for all infected classes. Nevertheless, a significantly higher fraction of asymptomatic chronic infected individuals (J_A) is observed for age group 2 compared to age group 1 relative to their fractions in I and I_A, which reinforces the importance of asymptomatic chronic infected adults.

In Figs. 2(a)–2(c), the curve for the total fractions (two age groups combined) for each of the infected classes and the curves in Fig. 3 will also be useful later for the comparison with the simulations with variable parameter values.

Figure 3 also shows how different $\mathcal{R}_0$ values affect the value at equilibrium (prevalence), and is therefore an indicator of what happens at the endemic state. For $\mathcal{R}_0 = 0.83 < 1$ the disease dies out as expected. For values of $\mathcal{R}_0 = 2, 3, 4, 5 > 1$, we reach after 25 years a non-trivial equilibrium. The prevalence of symptomatic children (Fig. 3(a)), asymptomatic children (Fig. 3(c)) and asymptomatic adults (Fig. 3(d)) decrease when $\mathcal{R}_0$ decreases. This can also be observed in Fig. 4, which shows $\mathcal{R}_0$ versus symptomatic and asymptomatic prevalence of age group 1 (plot (a)) and age group 2 (plot (b)). But it is interesting to notice that for the symptomatic adult population there is a slight increase in prevalence when lowering $\mathcal{R}_0$ (see Figs. 2(b) and 4(b) black curve). This indicates that a policy based solely on lowering $\mathcal{R}_0$ might come with a cost of appearance of symptomatic adult cases, which might need to be accounted for.

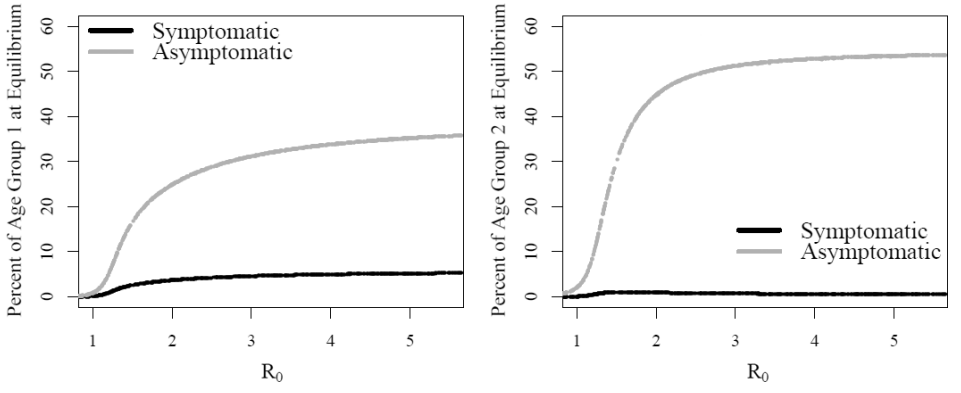

Fig. 4. The plots illustrate R_0 versus percent of age group 1 (plot (a)) and age group 2 (plot (b)) of symptomatic (black line) and asymptomatic (gray line) individuals, taken at equilibrium.

5.2.2. *Uncertainty analysis*

Although we have chosen the parameter values based on available information, it is important to examine how the uncertainty associated with the estimates of these parameter values may influence the model outcomes, such as the disease prevalence and the reproduction number. To do this, we consider a range of values for most of the parameters (as described in Table 2). Using a method based on Latin Hypercube Sampling, we simultaneously varied these parameters and performed uncertainty and sensitivity analyses. For the probability density function (pdf) used in Latin Hypercube Sampling, we used either a triangular (T) or uniform (U) distribution (see Table 2). For each pdf, we divided the parameter range into equally probable regions (one for each simulation), and sampled each region exactly once, creating a Latin Hypercube.[62,63] This statistical sampling method allows us to explore the dynamics of our model more efficiently and broadly than varying parameters individually, by using each parameter value chosen from the range only once in the simulations.[62] Our simulation results suggest that 1,000 sets of parameter values are enough to produce consistent results.

We conducted uncertainty analysis for the prevalence of malaria and for the reproduction number $\mathcal{R}_0$. To illustrate the variability in prevalence that results from uncertainty in the parameter values, we present in Figs. 5 and 6 the box plots of the fraction of individuals over time. Each plot divides the results of 1,000 simulations into quartiles at each moment in time, plotted every six months for 25 years. The median value is represented by the thicker curve and the box around the median value represents the interquartile range. The dotted lines extend to cover the 95% confidence interval for our outcome distributions. It shows a very similar trend among the 1,000 simulations, with the interquartile range having the same shape and a small range of values concentrated around the median. We can

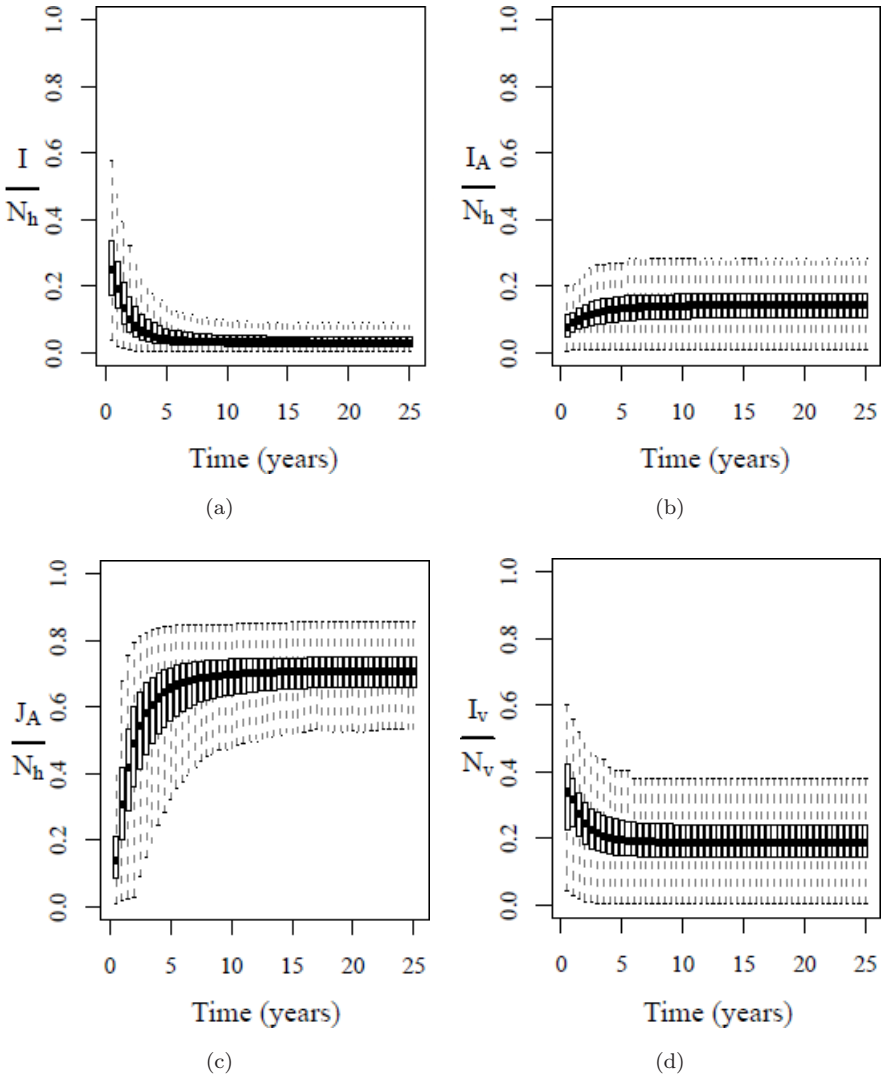

Fig. 5. Time-dependent uncertainty analysis with 1,000 simulations and parameter values from distributions given in Table 2. Plots in (a)–(c) illustrate time-dependent density distributions of the populations in the symptomatic infectious (I), asymptomatic infectious (I_A) and asymptomatic chronic infected (J_A) classes, respectively, and (d) shows the fraction of infectious mosquitoes. Each graph consists of boxplots plotted every six months for 25 years. The thick black curve is the median value and the interquartile range is the box around the median value. The dotted lines extend to cover the 95% confidence interval for our outcome distributions.

compare the median values from the uncertainty analysis in Figs. 5 and 6 with the simulation results presented in Figs. 2(a)–2(d) and 3 respectively, when fixed parameter values were used. We observe that the medians in the plots for I, I_A and J_A in Figs. 5(a)–5(c) and for I_1, I_2, $I_{A_1} + J_{A_1}$, $I_{A_2} + J_{A_2}$ in Fig. 6 are very close

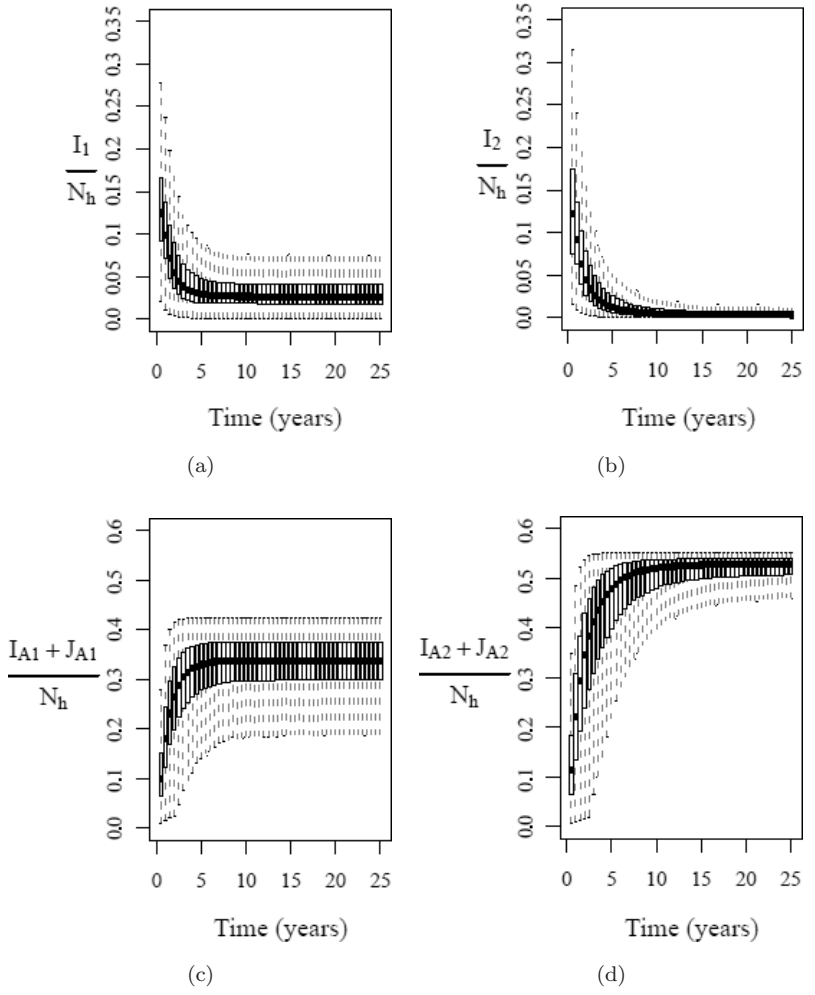

Fig. 6. Time-dependent uncertainty analysis with 1,000 simulations and parameter values from distributions given in Table 2. Plots (a) and (b) illustrate the time-dependent density distributions of the symptomatic infectious class for age groups 1 and 2, respectively, while (c) and (d) show that of the combined asymptomatic classes (asympt. infectious and asympt. chronic infected) for age groups 1 and 2, respectively. The thick black curve is the median value and the interquartile range is the box around the median value. The dotted lines extend to cover the 95% confidence interval for our outcome distributions.

to the corresponding curves in Figs. 2(a)–2(c) (see the thin curve) and the trend of the curves seen in Fig. 3 for $R_0 > 1$. This indicates that the choice of parameter ranges is robust.

Figures 7(a) and 7(b) are similar to Figs. 5 and 6 except that they provide information for the frequency distributions of infections at the endemic equilibrium (prevalence). For example, Fig. 7(a) shows the symptomatic prevalence in children

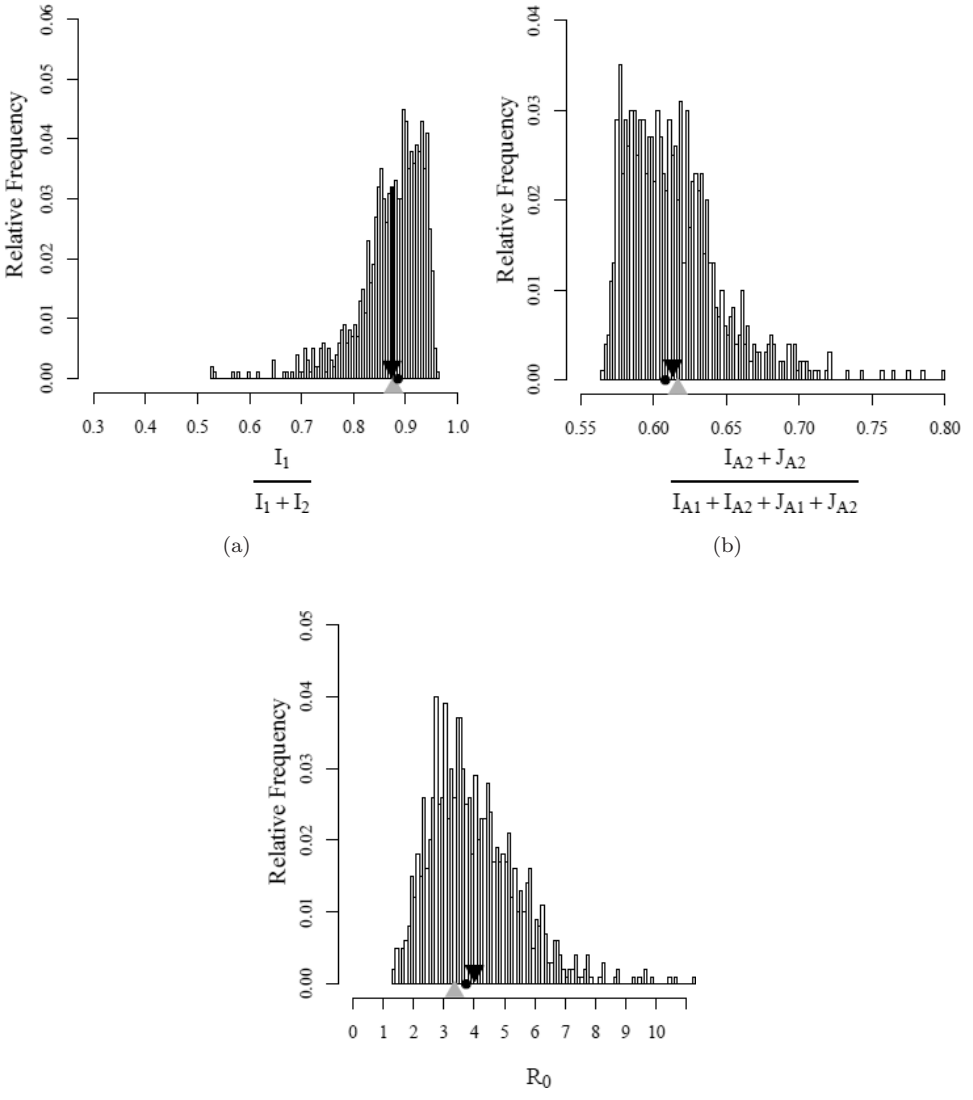

Fig. 7. Results of the uncertainty analysis from 1,000 simulations with variable parameter values for (a) the symptomatic prevalence in children relative to symptomatic prevalence, (b) asymptomatic infectious and asymptomatic chronic prevalence in adults relative to asymptomatic infectious and asymptomatic chronic prevalence, and (c) the reproduction number $\mathcal{R}_0$. The black triangle represents the mean prevalence in these 1,000 simulations with the median represented by a black dot, while the gray triangle indicates the prevalence from the fixed parameter setting. See text for more detailed explanations.

relative to the total symptomatic prevalence, $I_1/(I_1 + I_2)$, and Fig. 7(b) is for the asymptomatic prevalence in adults relative to the total asymptomatic prevalence, $(I_{A_2} + J_{A_2})/(I_{A_1} + J_{A_1} + I_{A_2} + J_{A_2})$. The black triangle labels the mean of the 1,000 simulations, and the gray triangle indicates the value from the simulations with fixed parameter values. The model predicts that among the symptomatic infections (I), children contribute to the majority of the cases (see Fig. 7(a)), which is concordant with collected observations.[46] We observe from Fig. 7(b) that adults form a majority of the asymptomatic infections ($I_A + J_A$), which is also consistent with reported data.[64] This again confirms that the model is capable of producing reasonable outcomes in terms of malaria prevalence.

Figure 7(c) illustrates the distribution of the values of the reproduction number $\mathcal{R}_0$ in the 1,000 simulations under the chosen parameter ranges. Let $\mathcal{R}_0^v$ denote the mean of the distribution (v for variable parameter values) and let $\mathcal{R}_0^f$ denote the reproduction number obtained when the fixed parameter values are used (f for fixed). The black triangle labels $\mathcal{R}_0^v = 4.01$ and the gray triangle indicates $\mathcal{R}_0^f = 3.4$. The relatively low variability of the distribution and the fact that $\mathcal{R}_0^v$ is very close to $\mathcal{R}_0^f$ indicate that the chosen parameter ranges are robust. Notice in Fig. 7 that in all simulations we have an $\mathcal{R}_0$ value greater than 1, indicating that malaria is likely to persist, as observed in malaria endemic regions.

5.2.3. *Sensitivity analysis*

To examine the sensitivity of the model outcomes (e.g., the reproduction number $\mathcal{R}_0$ and the time-dependent disease prevalence) to model parameters, we calculate partial rank correlation coefficients (PRCC) using the same 1,000 sets of parameter values. This statistical method produces a sensitivity index, which determines the effect of varying one parameter on the outcome while fixing other parameters at the expected value from their pdf.[62,63,65] These sensitivity indices have a value between -1 and 1. A positive (negative) PRCC indicates a positive (negative) relationship between the parameter and outcome. Furthermore, the absolute values of PRCC indices can help determine which parameter value(s) may have the strongest influence on the outcome variable, with a magnitude of 0 having almost no influence and 1 having the most influence.[62,63,65,66]

Figure 8 shows the PRCC for (a) the reproduction number $\mathcal{R}_0$, (b) combined symptomatic and asymptomatic infectious prevalence, (c) symptomatic prevalence alone, and (d) asymptomatic infectious prevalence alone.

First, we remark that disease-induced death (δ_1, δ_2) is not included in Fig. 8 since it had a minimal impact on all of the epidemiological outcomes. Next, we will give a brief description of the impact that parameter values have on each of the epidemiological outcomes based on Fig. 8 and how age of the human host plays a role.

The parameters which have the most influence on $\mathcal{R}_0$ can be observed in Fig. 8(a). The biting rate β influences $\mathcal{R}_0$ most, followed by k (symptomatic fraction

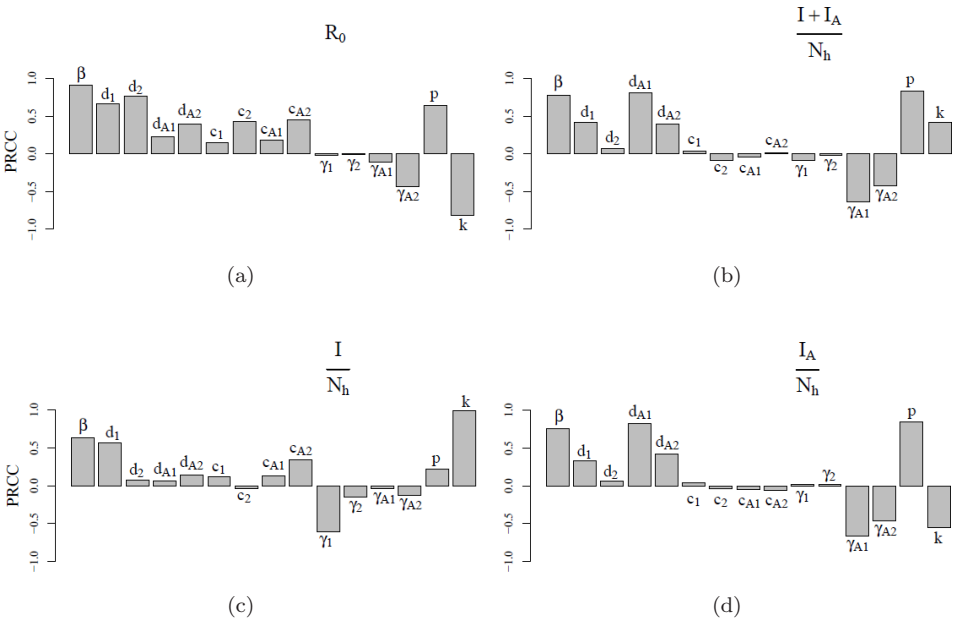

Fig. 8. Outcomes from the sensitivity analysis with parameter ranges defined in Table 2. PRCC for each parameter are plotted for four epidemiological outcomes: (a) $\mathcal{R}_0$, (b) overall infectious prevalence, (c) symptomatic prevalence, and (d) asymptomatic infectious prevalence. A larger absolute value of the PRCC indicates a greater impact on the epidemiological outcome, with positive (negative) values indicating a positive (negative) relationship.

after a susceptible individual becomes infected) and d_2 (probability of infection per bite in susceptible adults). It is important to notice that k affects $\mathcal{R}_0$ negatively, which may be counterintuitive. This is closely related to the unique feature in the model that chronically infected individuals may relapse when bitten by even susceptible mosquitoes. The intensity of the relapse depends heavily on the ratio of human to mosquito in addition to other parameters as indicated in the expression for $\mathcal{R}_0$ (see (4.31)). Such kind of negative relationship between $\mathcal{R}_0$ and k cannot be identified if the model does not consider relapse triggered by susceptible mosquitoes. The difference between age groups on the parameters that affect $\mathcal{R}_0$ can be observed by noticing that the magnitudes of PRCC of d_{A_2} and γ_{A_2} are larger than that of d_{A_1} and γ_{A_1}, respectively. This indicates that the $\mathcal{R}_0$ value is more strongly influenced by relapse of the adult group. The figure shows that in general infectiousness of individuals in the first age group (c_1, c_{A_1}) does not have as much influence over $\mathcal{R}_0$ as the infectiousness of those in the second age group (c_2, c_{A_2}). Last we can observe, that the difference in magnitude of d_1 and d_2 on the outcome $\mathcal{R}_0$ is not significant.

Figures 8(b)–8(d) show infectious prevalences of the disease. When considering the sensitivity of malaria prevalence to the change in parameters, the most

influential parameters identified may not be the same as the ones when sensitivity of $\mathcal{R}_0$ was being analyzed.

Figures 8(b) and 8(d) suggest that, for the overall infectious prevalence and asymptomatic infectious prevalence respectively, the most influential parameters are p (proportion of the year with high mosquito presence), d_{A_1} (probability of relapse of age group 1), followed by β. The parameter d_1 is noticeably more influential than its equivalent for age group 2 (d_2), as was not the case for $\mathcal{R}_0$, since in the case of $\mathcal{R}_0$, the susceptibility d_1 and d_2 of the two groups have a similar effect. In general, it is interesting to notice in Figs. 8(b) and 8(d), that most of the influential parameters correspond to age group 1. Moreover, the parameters with the most influence are the ones related to relapse. Also, infectiousness of humans to mosquitoes (i.e., c_i and c_{Ai}, $i = 1, 2$) as well as recovery rates ($\gamma_i, i = 1, 2$) have not a significant influence on the overall infectious and the asymptomatic infectious prevalence.

Finally, from Fig. 8(c) we observe that symptomatic prevalence is most sensitive to k, then β, followed closely by γ_1 (recovery rate of symptomatic children). It is surprising that the recovery rates γ_1 and γ_2 have dramatically different influence on symptomatic prevalence, with γ_1 having a much stronger impact. However, for the symptomatic prevalence, d_1 has a much stronger impact than d_2, as we could also observe for asymptomatic infectious and overall infectious prevalences and not for $\mathcal{R}_0$. Thus, the use of $\mathcal{R}_0$ as a measure for evaluation of policy decisions may not be optimal. It can also be observed for symptomatic prevalence that infectiousness of asymptomatic infectious adults (c_{A_2}) has a stronger positive impact than the other infectiousness parameters (c_1, c_2, c_{A_1}), which have a very small impact if at all.

Figures 9(a)–9(c) are similar to Figs. 8(b)–8(d), respectively, except that Fig. 9 shows the PRCC of the solution as a function of time. The total infectious fraction (see Fig. 9(a)) and the asymptomatic infectious fraction (see Fig. 9(c)) show similar trends and both are less variable, while the symptomatic infectious fraction (see Fig. 9(b)) shows noticeable fluctuations during the first 15 years in several parameters including β, γ_1, d_1 and d_2. We observe from Fig. 9(b) that, at the beginning of the simulation, β has a high positive impact (close to 1) on the symptomatic fraction. During the first 5 years, the PRCC of β decreases and starts to increase until the equilibrium level is reached after about 15 years. The two other influential parameters d_1 and d_2 also illustrate similar behavior; that is, the PRCC decreases during the initial 10 years of the simulation and then increases to reach the equilibrium level. However, the impact of d_1 on I is always positive, whereas the impact of d_2 is negative between approximately years 4 and 18, with the equilibrium level close to zero. The fluctuation behaviors suggest that, when implementing a control measure, it is best achieved when the fluctuations of the parameter are minimal. Notice that the constant effects of parameters on I_A (see Fig. 9(c)) dominate the effects on overall prevalence $I + I_A$ (see Fig. 9(a)), which again shows the importance of asymptomatic individuals in malaria prevalence and control.

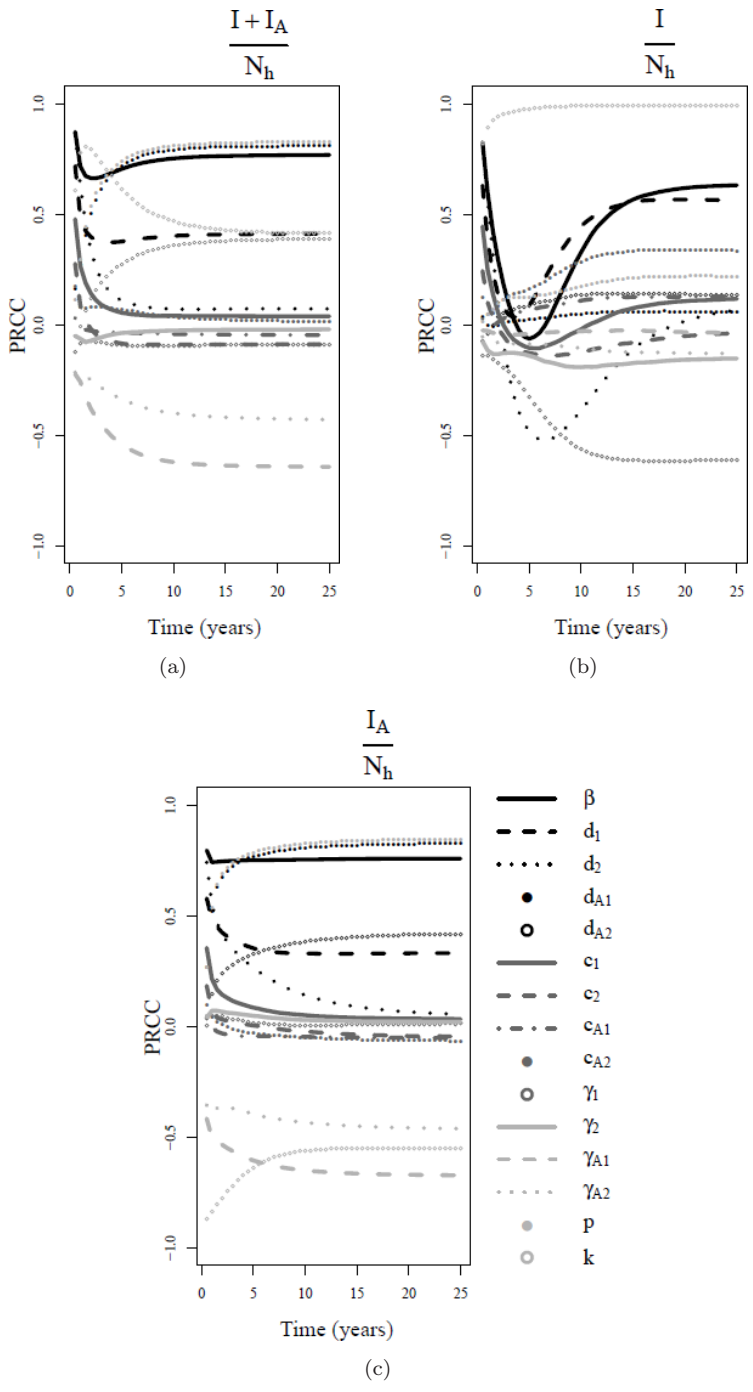

Fig. 9. Outcomes from the time-dependent sensitivity analysis with parameter ranges defined in Table 2. PRCC for each parameter are plotted over time for three outcomes: (a) overall prevalence, (b) symptomatic prevalence, and (c) asymptomatic prevalence.

6. Conclusion and Discussion

Eradication efforts in the past 30 years have failed to control malaria in many parts of Sub-Saharan Africa. An important factor of this failure is due to a poor understanding in the mechanisms of acquired immunity[5] as well as human behavior with respect to control measures.[67] The lack of understanding of how different types of immunity correlate and affect the disease dynamics has been an obstacle to the development of a malaria vaccine.[32] So far vector control measures have been successful but still do not seem to be sufficient. Vector control measures are part of the solution to control malaria but have to be applied in conjunction with human control measures and better implementation approaches. Although there have been mathematical models for the disease transmission dynamics of malaria focusing on various factors, to the best of our knowledge, none of the existing models consider all the relevant factors considered in our model. Immunity of human host to malaria infection has been modeled either as a separate epidemiological class or by considering loss of immunity for recovered individuals. These types of models do not specify which immunity is being referred to. We include chronological age of the human host, multiple types of age-dependent immunity (each represented by a specific parameter), asymptomatic infectious and asymptomatic chronic infected human classes, and relapse of chronic infected individuals triggered by susceptible mosquito bites as a reason for reappearance of gametocytemia, i.e., reappearance of human infectiousness. Our model allows the correlation between all these factors to play a role.

The model presented in this paper shows that asymptomatic infectious individuals contribute 2–3 times more than symptomatic individuals to malaria transmission. This indicates that control measures based on the information from reported clinical cases might not be adequate. This is well known in the malaria literature, but what has not been sufficiently studied yet is: where do so many asymptomatic infectious individuals come from? Is there a reservoir of asymptomatic chronic infected humans waiting to become infectious? Those questions are difficult to answer in field studies but need to be addressed. One hypothesis found in the literature is that reappearance of infectious asymptomatic individuals is triggered by even non-infectious mosquito bites. We included this hypothesis in our model and realized that it plays a fundamental role. The $\mathcal{R}_0$ expression is considerably affected by this assumption. This suggests that it is very important to further study the reasons for reappearance of gametocytemia, especially since many times public health decisions are based on $\mathcal{R}_0$.

It is known that low parasitemia and therefore asymptomatic chronic infections are difficult to measure. Our model produced the result that at least 60% of the population is asymptomatic chronic infected (not yet infectious), with twice as many adults than children. This means that this part of the population contributes to the infectious pool for mosquitoes, by eventually becoming asymptomatic infectious. This indicates as well, that the number of infected cases might be underestimated

in field studies and the utilization of more sensible measuring methods are strongly advised.

The structure of the model makes it also possible to investigate control measures that target a specific factor (represented by the parameters in our model).

We could observe some commonly expected results, e.g., that reducing the biting rate of mosquitoes (β) can have the most effective impact on the reduction of $\mathcal{R}_0$ as well as on the reduction of symptomatic, asymptomatic infectious and overall infectious prevalence. In addition to that, our model can also help determine the age group of humans to target for a specific type of vaccination and/or treatment implementation strategy, to achieve the most effective reduction in $\mathcal{R}_0$ and disease prevalence in the whole population. Most importantly, our model can help generate non-intuitive results.

For example, a pre-erythrocytic vaccine aims to generate antibodies responsible to neutralize sporozoites (stage of the parasite that goes from the mosquito saliva into the human body when bitten by an infectious mosquito).[32] This leads to a reduction in the probability of transmission from mosquitoes to susceptible humans and therefore the parameters that would be reduced by implementing a vaccine of this type are d_1 and d_2. Our simulation results show that by basing a Pre-erythrocytic vaccine implementation on $\mathcal{R}_0$ it would not be clear which age group to target, since the parameters d_1 and d_2 are almost equally impacting $\mathcal{R}_0$. If at all d_2 has a slightly more positive effect on $\mathcal{R}_0$ than d_1. But in fact, the best vaccination strategy would be to target children, i.e., lowering d_1, as the parameter d_1 has a significantly stronger positive effect on prevalence than d_2 (see Fig. 9), i.e., to target children would lower overall prevalence most efficiently. This provides an example for caution that in some cases a control measure determined based on $\mathcal{R}_0$ alone may not be optimal.

While vaccines targeting the pre-erythrocytic stages of the parasites would affect the infectiousness of humans indirectly, transmission-blocking vaccines aim to reduce infectiousness directly. These vaccines are based on antigens expressed on the surface of the sexual and mosquito mid-gut stages of malaria parasites. These antigens are the targets of antibodies induced by vaccination of the host and ingested with the parasites when a mosquito takes a blood meal. The antibodies act by inhibiting the parasite's development within the mosquito and thereby reduce the human infectiousness directly.[68] The parameters in our model related to transmission-blocking vaccines are c_1, c_2, c_{A_1} and c_{A_2} (probabilities of mosquito infection). Our results suggest that age group 2 (adults) should be targeted when implementing a transmission-blocking vaccine with focus on asymptomatic infectious adults (see Figs. 8(a) and 8(c)). To target asymptomatic infectious adults would effectively lower $\mathcal{R}_0$ as well as symptomatic prevalence.

As important as considering optimal vaccination strategies and vector control is effective treatment and diagnosis of malaria. Improving case management through strengthening health services in many countries is needed. Malaria control strongly

depends on correct diagnosis, prescription and availability of effective treatment.[69] Our results emphasize this and the importance of symptomatic children for malaria transmission. Our simulations show that the infectious period of symptomatic children (γ_1) has a significantly higher influence on the symptomatic prevalence than that of adults (γ_2). This suggests the importance to monitor the effective diagnosis and treatment especially for children, to reduce the symptomatic malaria prevalence efficiently.

We point out that many of the conclusions mentioned above depend critically on the rate of relapse triggered by mosquito bites on asymptomatic chronic individuals. A key parameter that determines the level of relapse is p, which depends on the length of time in a year when the mosquito density rises. Both $\mathcal{R}_0$ and the disease prevalence are very sensitive to the changes in p. A decrease in p (e.g., by reducing mosquito breeding sites when rainy season starts) will no doubt have a significant impact on malaria control as it will greatly reduce the influence of asymptomatic chronic humans on the overall malaria prevalence.

In summary, by incorporating several relevant factors such as relapse of asymptomatic chronic infected individuals triggered by non-infectious mosquitoes and different age-specific host immunity (anti-disease, anti-parasite and transmission-reducing immunity), our model is capable of generating important insights into the disease dynamics of malaria, which are not possible to obtain from existing models for malaria transmission. The model can be useful for evaluating the effectiveness of various control measures including vaccination and drug treatment for humans as well as vector control. The sensitivity and uncertainty analyses help identify the most influential factors for reducing the reproduction number $\mathcal{R}_0$ and the disease prevalence. The age-structure of the model makes it possible to determine specific age group(s) to target for vaccination or other control programs. We demonstrated the simulation results for the case of two age groups, since we found reasonable parameter values in the literature for 0–15 year old individuals. However, the model can be applied to any finite number of age groups. Although the model has already included many complexities associated with malaria transmission, there are assumptions made for simplicity. For example, p is taken constant but can be considered as a time-dependent function to allow for a seasonally variable relapse rate. Another extension would be to allow superinfection of asymptomatic chronic infected individuals, and, if at all realistic, to make k age dependent. We plan to consider these extensions in future studies.

Acknowledgments

We thank Carlos Castillo-Chavez for helpful suggestions. The modeling idea of this work started when KVG was a participant of the MTBI summer program at ASU. We thank Juan Cordovez Álvarez and Emmanuel Morales Butler for fruitful discussions during that summer. We would also like to thank the referees for their

valuable comments and suggestions. This work is partially supported by the NSF grant DMS-1022758.

References

1. CDC-(centers for disease control and prevention), November 29, 2012, Available at http://www.cdc.gov/malaria/about/index.html.
2. Nadjm B, Behrens RH, Malaria: An update for physicians, *Infect Dis Clin North Am* **26**(2):243–259, 2012.
3. WHO world health organization, January, 2013, Available at http://www.who.int/mediacentre/factsheets/fs094/en/index.html.
4. Sinka M, Bangs M, Manguin S, Coetzee M, Mbogo C, Hemingway J, Patil A, Temperley W, Gething P, Kabaria C, Okara R, Van Boeckel T, Godfray HC, Harbach R, Hay S, The dominant anopheles vectors of human malaria in Africa, Europe and the Middle East: Occurrence data, distribution maps and bionomic precis, *Parasit Vectors* **3**(1):117, 2010.
5. Doolan DL, Doban C, Baird JK, Aquired immunity to malaria, *Clin Microbiol Rev* **22**(1):13–36, 2009.
6. Bousema T, Interrupting malaria transmission: The effects of drugs and immunity on the transmissibility of Plasmodium falciparum, PhD Thesis, Radboud University Nijmegen, 2007.
7. Roird JK *et al.*, Age-dependent acquired protection against plasmodium falciparum in people having two years exposure to hyperendemic malaria, *Am J Trop Med Hyg* **45**(1):65–75, 1991.
8. Snow RW, Marsh K, New insights into the epidemiology of malaria relevant for disease control, *Br Med Bull* **54**(2):293–309, 1998.
9. Zurovac D, Larson BA, Skarbinski J, Slutsker L, Snow RW, Hamel MJ, Modeling the financial and clinical implications of malaria rapid diagnostic tests in the case-management of older children and adults in Kenya, *Am J Trop Med Hyg* **78**(6):884–891, 2008.
10. Baird JK, Age-dependent characteristics of protection v. susceptibility to plasmodium falciparum, *Ann Trop Med Parasitol* **92**:367–390, 1998.
11. Kurtis JD, Mtailb R, Onyango FK, Duffy PE, Human resistance to plasmodium falciparum increases during puberty and is predicted by dehydroepiandrosterone sulfate levels, *Infect Immun* **69**:123–128, 2001.
12. Dal-Bianco MP, Köster KB, Kombila UD, Kun JFJ, Grobusch MP, Ngoma GM, Matsiegui PB, Supan C, Ospina Salazar CL, Missinou MA *et al.*, High prevalence of asymptomatic plasmodium falciparum infection in gabonese adults, *Am J Trop Med Hyg* **77**(5):939–942, 2007.
13. Killeen GF, Ross A, Smith T, Infectiousness of malaria-endemic human populations to vectors, *Am J Trop Hyg* **75**(Suppl 2):38–45, 2006.
14. Drakeley C, Sutherland C, Bousema JT, Sauerwein RW, Targett GAT, The epidemiology of plasmodium falciparum gametocytes: Weapons of mass dispersion, *Trends Parasitol* **22**(9):424–430, 2006.
15. Bousema T, Drakeley C, Epidemiology and infectivity of plasmodium falciparum and plasmodium vivax gametocytes in relation to malaria control and elimination, *Clin Microbiol Rev* 377–410, 2011.
16. Paul REL, Diallo M, Brey PT, Mosquitoes and transmission of malaria parasites — not just vectors, *Malar J* **3**(39), 2004.

17. Lawaly R, Konate L *et al.*, Impact of mosquito bites on asexual parasite density and gametocyte prevalence in asymptomatic chronic plasmodium falciparum infections and correlation with ige and igg titers, *Infec Immun* **80**(6):2240–2246, 2012.
18. Ross R, *The Prevention of Malaria*, John Murray, London, 1911.
19. Mandal S, Rup Sarkar R, Sinha S, Mathematical models of malaria — a review, *Malar J* **10**(1):202, 2011.
20. May RM, Anderson RM, *Infectious Diseases of Humans: Dynamics and Control*, Oxford University Press, London, 1991.
21. Aron JL, May RM, The population dynamics of malaria, in Anderson RM (ed.), *Population Dynamics of Infectious Disease*, Chapman and Hall, London, 1982, pp. 139–179.
22. Dietz K, Mathematical models for transmission and control of malaria, in Wernsdorfer WH, McGregor (eds.) *Principles and Practice of Malariology*, Churchill Livingston, Edingburgh, 1988, pp. 1091–1133.
23. Aron JL, Mathematical modeling of immunity to malaria, *Math Biosci* **90**:385–396, 1988.
24. Filipe *et al.*, Determination of the processes driving the acquisition of immunity to malaria using a mathematical transmission model, *PloS Comp Biol* **3**:2569–2579, 2007.
25. Hasibeder G, Dey C, Population dynamics of mosquito-borne disease: Persistence ina completely heterogeneous environment, *Theor Popul Biol* **33**:31–53, 1988.
26. Chitnis N, Cushing JM, Hyman JM, Bifurcation analysis of a mathematical model for malaria transmission, *SIAM J Appl Math* **67**(1):24–45, 2006.
27. Sharma SK *et al.*, Epidemiology of malaria transmission and development of natural immunity in a malaria-endemic village, San Dulakudar, in Orissa State, India, *Am J Trop Med Hyg* **71**(9), 2004.
28. Ladeia-Andrade S *et al.*, Age-dependent acquisition of protective immunity to malaria in riverine populations of the amazon basin of brazil, *Am J Trop Med Hyg* **80**:452–459, 2009.
29. Boyd MF, Epidemiology of malaria: Factors related to the intermediate host, *Malariology*, 551–607, 1949.
30. Dietz K, Molineaux L, Thomas A, A malaria model tested in the African savannah, *Bull World Health Organ* **50**:347–357, 1974.
31. Ngwa GA, Shu WS, A mathematical model for endemic malaria with variable human and mosquito populations, *Math Comput Model* **32**(78):747–763, 2000.
32. Girard MP, Reed ZH, Friede M, Kieny MP, A review of human vaccine research and development: Malaria, *Vaccine* **25**(9):1567–1580, 2007.
33. van den Driessche P, Watmough J, Reproduction numbers and sub-threshold endemic equilibria for compartmental models of disease transmission, *Math Biosci* **180**:29–48, 2002.
34. Hadeler KP, Müller J, Vaccination in age structured populations I: The reproduction number, in Isham V, *et al.* (eds.), *Epidemic Models*: *Their Structure and Relation to Data*, Cambridge University, Cambridge, p. 90, 1996.
35. Hadeler KP, Müller J, Vaccination in age structured populations II: Optimal strategies, in Isham V, *et al.* (eds.), *Models for Infectious Human Diseases: Their Structure and Relation to Data*, Cambridge University Press, Cambridge, pp. 102–114, 1996.
36. Iannelli M, *Mathematical Theory of Age-Structured Population Dynamics*, Giardini Editori E Stampatori, Pisa, 1995.
37. Thieme HR, Convergence results and a poincare-bendixon trichotomy for asymptotically autonomous differential equations, *J Math Biol* **30**:755–763, 1992.

38. Castillo-Chavez C, Feng Z, Global stability of an age-structure model for TB and its applications to optimal vaccination, *Math Biosci* **151**:135–154, 1998.
39. Shim E, Feng Z, Martcheva M, Castillo-Chavez C, An age-structured epidemic model of rotavirus with vaccination, *J Math Biol* **53**(4):719–746, 2006.
40. Hethcote HW, The mathematics of infectious diseases, *SIAM Rev* **42**(4):599–653, 2000.
41. R Development Core Team, *R: A Language and Environment for Statistical Computing*, R Foundation for Statistical Computing, Vienna, Austria, 2011.
42. United Nations, Department of Economic and Social Affairs, Population Division, Population Estimates and Projections Sections, January, 2013, Available at http://esa.un.org/wpp/index.htm.
43. Presidents malaria initiative, Tanzania, malaria operational plan fy 2013, January, 2013, Available at http://pmi.gov/countries/profiles/tanzania.html.
44. Craig MH, Snow RW, le Sueur D, A climate-based distribution model of malaria transmission in sub-saharan Africa, *Parasitol. Today* **15**(3):755–763, 1999.
45. Trape JF, Zoulani A, Quinet MC, Assessment of the incidence and prevalence of clinical malaria in semi-immune children exposed to intense and perennial transmission, *Am J Epidemiol* **126**(2):193–201, 1987.
46. Reyburn H, Mbatia R, Drakeley C *et al.*, Association of transmission intensity and age with clinical manifestations and case fatality of severe plasmodium falciparum malaria, *JAMA* **293**(12):1461–1470, 2005.
47. White NJ, Hoffman S, Campbell CC, Malaria, in *Tropical Infectious Diseases. Principles, Pathogens and Practice*, Elsevier Churchill Livingstone, Philadelpia, pp. 1024–1062, 2006.
48. Greenwood B, Marsh K, Snow R, Why do some African children develop severe malaria? *Parasitol Today* **7**(10):277–281, 1991.
49. Kwiatkowski DP, How malaria has affected the human genome and what human genetics can teach us about malaria, *Am J Hum Genet* **77**(2):171–192, 2005.
50. Dolo, A, Modiano D, Maiga B, Daou M, Dolo G, Guindo H, Ba M, Maiga H, Coulibaly D, Perlman H *et al.*, Difference in susceptibility to malaria between two sympatric ethnic groups in mali, *Am J Trop Med Hyg* **72**(3):243–248, 2005.
51. Baird JK, Jones TR, Danudirgo EW, Annis BA, Bangs MJ, Basri PH, Masbar S, Age-dependent acquired protection against plasmodium falciparum in people having two years exposure to hyperendemic malaria, *Am J Trop Med Hyg* **45**(1):65–76, 1991.
52. Targett GA *et al.*, Plasmodium falciparum: Natural and experimental transmission-blocking immunity, *Immunol Lett* **19**(3):235, 1988.
53. Drakeley CJ, Bousema JT, Akim NIJ, Teelen K, Roeffen W, Lensen AH, Bolmer M, Eling W, Sauerwein RW, Transmission-reducing immunity is inversely related to age in plasmodium falciparum gametocyte carriers, *Parasite Immunol* **28**(5):185–190, 2006.
54. Miller MJ, Observations on the natural history of malaria in the semi-resistant West African, *Trans R Soc Trop Med Hyg* **52**(2):152–168, 1958.
55. Gouagna LC, Ferguson HM, Okech BA, Killeen GF, Kabiru EW, Beier JC, Githure JI, Yan G, Plasmodium falciparum malaria disease manifestations in humans and transmission to anopheles gambiae: A field study in western Kenya, *Parasitology* **128**(03):235–243, 2004.
56. Bruce MC, Donnelly CA, Packar M, Lagog M, Gibson N, Narara A, Walliker D, Alpers MP, Day KP, Age- and species-specific duration of infection in asymptomatic malaria infections in papua new guinea, *Parasitology* **121**:247–256, 2000.

57. Bousema J, Gouagna L, Drakeley C, Meutstege A, Okech B, Akim I, Beier J, Githure J, Sauerwein R, Plasmodium falciparum gametocyte carriage in asymptomatic children in western Kenya, *Malar J* **3**(1):18, 2004.
58. Garret-Jones C, Shidrawi GR, Malaria vectorial capacity of a population of anopheles gambiae, *Bull Wld Hlth Org* **40**:531–545, 1969.
59. Paaijmans K, Weather, water and malaria mosquito larvae, 2008.
60. Chitnis N, Hyman JM, Cushing JM, Determining important parameters in the spread of malaria through the sensitivity analysis of a mathematical model, *Bull Math Biol* **70**:1272–1296, 2008.
61. Laishram DD, Sutton PL, Nanda N, Sharma VL, Sobti RC, Carlton JM, Joshi H *et al.*, The complexities of malaria disease manifestations with a focus on asymptomatic malaria, *Malar J* **11**(1):29, 2012.
62. Blower SM, Dowlatabadi H, Sensitivity and uncertainty analysis of complex models of disease transmission: An HIV model, as an example, *Int Stat Rev* 229–243, 1994.
63. Helton JC, Johnson JD, Sallaberry CJ, Storlie CB, Survey of sampling-based methods for uncertainty and sensitivity analysis, *Reliab Eng Syst Safe* **91**(10):1175–1209, 2006.
64. Alves FP, Gil LHS, Marrelli MT, Ribolla PEM, Camargo EP, Da Silva LHP, Asymptomatic carriers of Plasmodium spp. as infection source for malaria vector mosquitoes in the brazilian amazon, *J Med Entomol* **42**(5):777–779, 2005.
65. Hamby DM, A review of techniques for parameter sensitivity analysis of environmental models, *Environ Monit Assess* **32**(2):135–154, 1994.
66. Blower SM, Porco TC, Darby G, Predicting and preventing the emergence of antiviral drug resistance in hsv-2, *Nat Med* **4**(6):673–678, 1998.
67. Aguto FB, Del Valle SY, Blayneh KW, Ngonghala CN *et al.*, The impact of bed-net use on malaria prevalence, *J Theor Biol* **320**:58–65, 2013.
68. Carter R, Stowers A, Current developments in malaria transmission-blocking vaccines, *Expert Opin Biol Ther* **1**(4):619–628, 2001. PMID: 11727498.
69. Font F, Alonso Gonzlez M, Nathan R, Kimario J, Lwilla F, Ascaso C, Tanner M, Menndez C, Alonso PL, Diagnostic accuracy and case management of clinical malaria in the primary health services of a rural area in south-eastern Tanzania, *Trop Med Int Health* **6**(6):423–428, 2001.

Appendix A

In this appendix we give the proof of Theorem 3.1.

Proof. Consider first the case when $\omega \in \mathbb{R}$. Notice that

$$\frac{\partial}{\partial\omega}F(a,\omega) = \int_0^a \bar{\lambda}_1(\sigma)(\sigma-a)\mathrm{e}^{-\int_\sigma^a(\gamma(\tau)+\mu(\tau)+\delta(\tau)+\omega)d\tau}d\sigma < 0,$$

$$\begin{aligned}\frac{\partial}{\partial\omega}G(a,\omega,p) = \int_0^a \Bigg\{ & p\bar{\lambda}_2(\sigma)\int_0^\sigma [\bar{\lambda}_1(\xi)(\xi-\sigma)\mathrm{e}^{-\int_\xi^\sigma(\mu(\tau)+\omega)d\tau}]d\xi P_A(a,\sigma,\omega) \\ & + \left[\bar{\lambda}_1(\sigma)+p\bar{\lambda}_2(\sigma)\int_0^\sigma \bar{\lambda}_1(\xi)\mathrm{e}^{-\int_\xi^\sigma(\mu(\tau)+\omega)d\tau}d\xi\right](\sigma-a)P_A(a,\sigma,\omega)\Bigg\}d\sigma \\ & < 0\end{aligned}$$

as $\xi - \sigma < 0$ and $\sigma - a < 0$. Thus,

$$\begin{aligned}\Theta'(\omega) &= -\frac{\bar{\lambda}_v}{(\omega+\mu_v)^2}\left[\int_0^\infty c_A(a)(1-k)G(a,\omega,p)da + \int_0^\infty c(a)kF(a,\omega)da\right] \\ &\quad + \frac{\bar{\lambda}_v}{\omega+\mu_v}\left[\int_0^\infty c_A(a)(1-k)\frac{\partial G}{\partial \omega}da + \int_0^\infty c(a)k\frac{\partial F}{\partial \omega}da\right] \\ &< 0\end{aligned}$$

and $\Theta(\omega)$ is a continuous decreasing function. Moreover, since $F(a,\omega) \to 0$ and $G(a,\omega,p) \to 0$ as $\omega \to \infty$, it is easy to see that $\lim_{\omega\to\infty}\Theta(\omega) = 0$. Similarly, it can also be shown easily that $\lim_{\omega\to-\infty}\Theta(\omega) = \infty$. Therefore, there exists a unique real root, denoted by ω_0, of the characteristic equation $\Theta(\omega) = 1$ such that $\Theta(\omega) > 1$ (<1) for $\omega < \omega_0$ ($>\omega_0$).

Next we show that when $\omega_0 < 0$, all complex solutions of the equation $\Theta(\omega) = 1$ will have a negative real part. Let $z \in \mathbb{C}$ and $\Theta(z) = 1$. If $\mathrm{Re}\{z\} \geq 0$, then

$$\begin{aligned}\Theta(\omega_0) = 1 &= |\Theta(z)| \\ &\leq \frac{\bar{\lambda}_v}{\mathrm{Re}\{z\}+\mu_v}\left[\int_0^\infty c_A(a)(1-k)G(a,\mathrm{Re}\{z\},p)da + \int_0^\infty c(a)kF(a,\mathrm{Re}\{z\})da\right] \\ &= \Theta(\mathrm{Re}\{z\}).\end{aligned}$$

Since $\Theta(\omega)$ is a decreasing function, from the above inequality we have $\mathrm{Re}\{z\} \leq \omega_0$, which is a contradiction. This implies that $\mathrm{Re}\{z\} < 0$ whenever $\omega_0 < 0$.

Note that $\mathcal{R}_0 := \Theta(0)$. Thus, $\omega_0 < 0$ (>0) if $\mathcal{R}_0 < 1$ (>1). It follows that the disease-free state E^* is locally asymptotically stable if $\mathcal{R}_0 < 1$ and unstable if $\mathcal{R}_0 > 1$. This completes the proof. □

Appendix B

In this appendix, we include the details for the derivation of the reproduction number $\mathcal{R}_0$ for the cases of one and two age groups.

B.1. *The case of $n = 1$ age group*

Noticing that $\alpha_1 = 0$ the matrices F and V reduce to:

$$F = \begin{pmatrix} 0 & 0 & 0 & k\beta\dfrac{d_1}{\bar{N}_h}\bar{N}_1 \\ 0 & 0 & 0 & (1-k)\beta\dfrac{d_1}{\bar{N}_h}\bar{N}_1 \\ 0 & 0 & 0 & 0 \\ \beta c_1\dfrac{\bar{N}_v}{\bar{N}_h} & \beta c_{A1}\dfrac{\bar{N}_v}{\bar{N}_h} & 0 & 0 \end{pmatrix},$$

$$V = \begin{pmatrix} \bar{\gamma}_1 & 0 & 0 & 0 \\ 0 & \bar{\gamma}_{A_1} & -p\beta d_{A1}\dfrac{\bar{N}_v}{\bar{N}_h} & 0 \\ 0 & -\gamma_{A1} & p\beta d_{A1}\dfrac{\bar{N}_v}{\bar{N}_h} + \mu_1 & 0 \\ 0 & 0 & 0 & \mu_v \end{pmatrix} \tag{B.1}$$

from which we get

$$V^{-1} = \begin{pmatrix} T_1 & 0 & 0 & 0 \\ 0 & \dfrac{1}{\mu_1}\dfrac{\mu_1 + p\beta d_{A_1}\frac{\bar{N}_v}{\bar{N}_h}}{\bar{\gamma}_{A_1} + p\beta d_{A_1}\frac{\bar{N}_v}{\bar{N}_h}} & \dfrac{1}{\mu_1}\dfrac{p\beta d_{A_1}\frac{\bar{N}_v}{\bar{N}_h}}{\bar{\gamma}_{A_1} + p\beta d_{A_1}\frac{\bar{N}_v}{\bar{N}_h}} & 0 \\ 0 & \dfrac{1}{\mu_1}\dfrac{\gamma_{A_1}}{\bar{\gamma}_{A_1} + p\beta d_{A_1}\frac{\bar{N}_v}{\bar{N}_h}} & \dfrac{1}{\mu_1}\dfrac{\bar{\gamma}_{A_1}}{\bar{\gamma}_{A_1} + p\beta d_{A_1}\frac{\bar{N}_v}{\bar{N}_h}} & 0 \\ 0 & 0 & 0 & \dfrac{1}{\mu_v} \end{pmatrix}. \tag{B.2}$$

Thus,

$$FV^{-1} = \begin{pmatrix} 0 & 0 & 0 & \dfrac{k\beta d_1}{\bar{N}_h}\bar{N}_1 T_v \\ 0 & 0 & 0 & \dfrac{(1-k)\beta d_1}{\bar{N}_h}\bar{N}_1 T_v \\ 0 & 0 & 0 & 0 \\ \beta c_1 \dfrac{\bar{N}_v}{\bar{N}_h} T_1 & \dfrac{\mu_1 + p\beta d_{A_1}\frac{\bar{N}_v}{\bar{N}_h}}{\bar{\gamma}_{A_1} + p\beta d_{A_1}\frac{\bar{N}_v}{\bar{N}_h}}\dfrac{\beta c_{A_1}\frac{\bar{N}_v}{\bar{N}_h}}{\mu_1} & \dfrac{p\beta d_{A_1}\frac{\bar{N}_v}{\bar{N}_h}}{\bar{\gamma}_{A_1} + p\beta d_{A_1}\frac{\bar{N}_v}{\bar{N}_h}}\dfrac{\beta c_{A_1}\frac{\bar{N}_v}{\bar{N}_h}}{\mu_1} & 0 \end{pmatrix} \tag{B.3}$$

which is the same as the FV^{-1} matrix in (4.27).

For the explanation of $P_{I_{A_1}}^{I_{A_1}}$ we let $q_1 = \gamma_{A_1}/(\gamma_{A_1} + \mu_1) = \gamma_{A_1}/\bar{\gamma}_{A_1}$ denote the probability that a person in I_{A_1} moves to J_{A_1}, let $q_2 = \rho_1/(\rho_1 + \mu_1)$ denote the probability that a person in J_{A_1} moves back to I_{A_1}, where $\rho_1 = p\beta d_{A_1}\bar{N}_v/\bar{N}_h$, and let $q_3 = \mu_1/\bar{\gamma}_{A_1}$ denote the probability that once in I_A a person does not return to J_A. Then, the probability that a person who starts in I_{A_1} and returns to I_{A_1} after visiting J_{A_1} exactly one time is $q_1q_2q_3$, exactly twice is $(q_1q_2)^2q_3$, and exactly k times is $(q_1q_2)^kq_3$, $k = 1, 2, \ldots$. Then, the probability that a person is in I_{A_1}, given that the person entered the $I_{A_1} \leftrightarrows J_{A_1}$ loop through I_{A_1}, is

$$P_{I_{A_1}}^{I_{A_1}} = \sum_{k=0}^{\infty}(q_1q_2)^kq_3 = q_3\sum_{k=0}^{\infty}(q_1q_2)^k = \frac{\mu_1}{\bar{\gamma}_{A_1}}\frac{\bar{\gamma}_{A_1}(\rho_1+\mu_1)}{\mu_1(\rho_1+\bar{\gamma}_{A_1})} = \frac{\rho_1+\mu_1}{\rho_1+\bar{\gamma}_{A_1}}. \tag{B.4}$$

B.2. *The case of $n = 2$ age groups*

In this case $\alpha_2 = 0$, and the F and V matrices are given by:

$$F = \begin{pmatrix} 0 & 0 & 0 & 0 & k\beta\dfrac{d_1}{\bar{N}_h}\bar{N}_1 \\ 0 & 0 & 0 & 0 & \mathbf{h}_{A_1} \\ 0 & 0 & 0 & 0 & k\beta\dfrac{d_2}{\bar{N}_h}\bar{N}_2 \\ 0 & 0 & 0 & 0 & \mathbf{h}_{A_2} \\ \beta c_1\dfrac{\bar{N}_v}{\bar{N}_h} & \mathbf{v}_{A_1} & \beta c_2\dfrac{\bar{N}_v}{\bar{N}_h} & \mathbf{v}_{A_2} & 0 \end{pmatrix}, \tag{B.5}$$

$$V = \begin{pmatrix} \bar{\gamma}_1 & 0 & 0 & 0 & 0 \\ 0 & \mathcal{A}_{A_1} & 0 & 0 & 0 \\ -\alpha_1 & 0 & \bar{\gamma}_2 & 0 & 0 \\ 0 & -\mathcal{C}_1 & 0 & \mathcal{A}_{A_2} & 0 \\ 0 & 0 & 0 & 0 & \mu_v \end{pmatrix},$$

where

$$\mathbf{h}_{A_1} = \begin{pmatrix} \beta\dfrac{d_1}{\bar{N}_h}\bar{N}_1 \\ 0 \end{pmatrix}, \quad \mathbf{h}_{A_2} = \begin{pmatrix} \beta\dfrac{d_2}{\bar{N}_h}\dfrac{\Lambda}{\mu_2}\dfrac{\alpha_1}{\alpha_1+\mu_1} \\ 0 \end{pmatrix}, \tag{B.6}$$

$$\mathbf{v}_{A_1} = \left(\beta c_{A_1}\frac{\bar{N}_v}{\bar{N}_h}, 0\right), \quad \mathbf{v}_{A_2} = \left(\beta c_{A_2}\frac{\bar{N}_v}{\bar{N}_h}, 0\right), \tag{B.7}$$

$$\mathcal{A}_{A_1} = \begin{pmatrix} \bar{\gamma}_{A_1} & -p\beta d_{A_1}\dfrac{\bar{N}_v}{\bar{N}_h} \\ -\gamma_{A_1} & p\beta d_{A_1}\dfrac{\bar{N}_v}{\bar{N}_h} + \mu_1 + \alpha_1 \end{pmatrix}, \quad \mathcal{A}_{A_2} = \begin{pmatrix} \bar{\gamma}_{A_2} & -p\beta d_{A_2}\dfrac{\bar{N}_v}{\bar{N}_h} \\ -\gamma_{A_2} & p\beta d_{A_2}\dfrac{\bar{N}_v}{\bar{N}_h} + \mu_2 \end{pmatrix}, \tag{B.8}$$

$$\mathcal{C}_1 = \begin{pmatrix} \alpha_1 & 0 \\ 0 & \alpha_1 \end{pmatrix}. \tag{B.9}$$

Note that

$$V^{-1} = \begin{pmatrix} T_1 & 0 & 0 & 0 & 0 \\ 0 & \mathcal{A}_{A_1}^{-1} & 0 & 0 & 0 \\ \dfrac{\theta_1}{\gamma_2} & 0 & T_2 & 0 & 0 \\ 0 & \mathcal{A}_{A_2}^{-1}\mathcal{C}_1\mathcal{A}_{A_1}^{-1} & 0 & \mathcal{A}_{A_2}^{-1} & 0 \\ 0 & 0 & 0 & 0 & T_v \end{pmatrix}, \tag{B.10}$$

where

$$\mathcal{A}_{A_1}^{-1} = \frac{1}{\mu_1+\alpha_1}\begin{pmatrix} \dfrac{p\beta d_{A_1}\frac{\bar{N}_v}{\bar{N}_h}+\mu_1+\alpha_1}{\bar{\gamma}_{A_1}+p\beta d_{A_1}\frac{\bar{N}_v}{\bar{N}_h}} & \dfrac{p\beta d_{A_1}\frac{\bar{N}_v}{\bar{N}_h}}{\bar{\gamma}_{A_1}+p\beta d_{A_1}\frac{\bar{N}_v}{\bar{N}_h}} \\ \dfrac{\gamma_{A_1}}{\bar{\gamma}_{A_1}+p\beta d_{A_1}\frac{\bar{N}_v}{\bar{N}_h}} & \dfrac{\bar{\gamma}_{A_1}+\alpha_1}{\bar{\gamma}_{A_1}+p\beta d_{A_1}\frac{\bar{N}_v}{\bar{N}_h}} \end{pmatrix}, \tag{B.11}$$

$$\mathcal{A}_{A_2}^{-1} = \frac{1}{\mu_2}\begin{pmatrix} \dfrac{p\beta d_{A_2}\frac{\bar{N}_v}{\bar{N}_h}+\mu_2}{\bar{\gamma}_{A_2}+p\beta d_{A_2}\frac{\bar{N}_v}{\bar{N}_h}} & \dfrac{p\beta d_{A_2}\frac{\bar{N}_v}{\bar{N}_h}}{\bar{\gamma}_{A_2}+p\beta d_{A_2}\frac{\bar{N}_v}{\bar{N}_h}} \\ \dfrac{\gamma_{A_2}}{\bar{\gamma}_{A_2}+p\beta d_{A_2}\frac{\bar{N}_v}{\bar{N}_h}} & \dfrac{\bar{\gamma}_{A_2}}{\bar{\gamma}_{A_2}+p\beta d_{A_2}\frac{\bar{N}_v}{\bar{N}_h}} \end{pmatrix}. \tag{B.12}$$

Thus,

$$FV^{-1} = \begin{pmatrix} 0 & 0 & 0 & 0 & k\frac{\beta d_1}{\bar{N}_h}\bar{N}_1 T_v \\ 0 & 0 & 0 & 0 & (1-k)\hbar_{A_1}T_v \\ 0 & 0 & 0 & 0 & k\frac{\beta d_2}{\bar{N}_h}\bar{N}_2 T_v \\ 0 & 0 & 0 & 0 & (1-k)\hbar_{A_2}T_v \\ \beta c_1\frac{\bar{N}_v}{\bar{N}_h}T_1+\theta\beta c_2\frac{\bar{N}_v}{\bar{N}_h}T_2 & v_{A_1}\mathcal{A}_{A_1}^{-1}+v_{A_2}\mathcal{A}_{A_2}^{-1}\mathcal{C}_1\mathcal{A}_{A_1}^{-1} & \frac{\beta c_2\frac{\bar{N}_v}{\bar{N}_h}}{\bar{\gamma}_2} & v_{A_2}\mathcal{A}_{A_2}^{-1} & 0 \end{pmatrix} \tag{B.13}$$

which is the same as (4.30). It follows that

$$\begin{aligned} -E_2(FV^{-1}) = {} & k\frac{\beta d_1}{\bar{N}_h}\bar{N}_1 T_v\left(\beta c_1\frac{\bar{N}_v}{\bar{N}_h}T_1+\theta_1\beta c_2\frac{\bar{N}_v}{\bar{N}_h}T_2\right)+k\frac{\beta d_2}{\bar{N}_h}\bar{N}_2 T_v\beta c_2\frac{\bar{N}_v}{\bar{N}_h}T_2 \\ & +(v_{A_1}\cdot\mathcal{A}_{A_1}^{-1}+v_{A_2}\cdot\mathcal{A}_{A_2}^{-1}\mathcal{C}_1\mathcal{A}_{A_1}^{-1})\hbar_{A_1}T_v+v_{A_2}\cdot\mathcal{A}_{A_2}^{-1}\hbar_{A_2}T_v. \end{aligned} \tag{B.14}$$

This leads to the formula for $\mathcal{R}_0 = \sqrt{-E_2(FV^{-1})}$ given in (4.31).

The following shows the explanation of the expressions in (4.32)–(4.34).

For the explanation of $P_{I_{A_k}}^{I_{A_k}}$ in (4.32) ($k = 1, 2$), we let $q_{1k} = \gamma_{A_k}/\bar{\gamma}_{A_k}$ denote the probability that a person in I_{A_k} moves to J_{A_k} and $q_{2k} = \rho_k/(\rho_k+\mu_k+\alpha_k)$ the probability that a person in J_{A_k} moves back to I_{A_k}. Let $q_{3k} = (\mu_k+\alpha_k)/(\bar{\gamma}_{A_k})$ denote the probability that once in I_{A_k} a person does not return to J_{A_k}. Then, the derivation of the expression in (4.32) for $P_{I_{A_k}}^{I_{A_k}}$ is equivalent as explained in the case for $n = 1$ age groups.

For the explanation of $P_{I_{A_1}}^{J_{A_1}}$ in (4.33), we let $q_1 = \gamma_{A_1}/\bar{\gamma}_{A_1}$ denote the probability that a person in I_{A_1} moves to J_{A_1} and $q_2 = \rho_1/(\rho_1+\mu_1+\alpha_1)$ the probability that a person in J_{A_1} moves back to I_{A_1}. Let $p_3 = (\mu_1+\alpha_1)/(\rho_1+\mu_1+\alpha_1)$ denote the probability that once in J_{A_1} a person does not return to I_{A_1}. Then the probability

that a person is in J_{A_1}, given that the person entered the $I_{A_1} \leftrightarrows J_{A_1}$ loop through I_{A_1}, is given by

$$P_{I_{A_1}}^{J_{A_1}} = \sum_{k=1}^{\infty}(q_1)^k(q_2)^{k-1}p_3 = p_3\sum_{k=1}^{\infty}(q_1)^k(q_2)^{k-1}$$

$$= \frac{\mu_1+\alpha_1}{\rho_1+\mu_1+\alpha_1}\frac{\gamma_{A_1}}{\bar{\gamma}_{A_1}}\frac{\bar{\gamma}_{A_1}(\rho_1+\mu_1+\alpha_1)}{(\mu_1+\alpha_1)(\rho_1+\bar{\gamma}_{A_1})} = \frac{\gamma_{A_1}}{\rho_1+\bar{\gamma}_{A_1}}. \tag{B.15}$$

For the explanation of $P_{J_{A_2}}^{I_{A_2}}$ in (4.34), we let $q_1 = \gamma_{A_2}/\bar{\gamma}_{A_2}$ denote now the probability that a person in I_{A_2} moves to J_{A_2} and $q_2 = \rho_2/(\rho_2+\mu_2)$ the probability that a person in J_{A_2} moves back to I_{A_2}. Let $p_3 = \mu_2/(\gamma_{A_2}+\mu_2)$ denote the probability that once in I_{A_2} a person does not return to J_{A_2}. Then the probability that a person is in I_{A_2} if that person entered the $I_{A_2} \leftrightarrows J_{A_2}$ loop through J_{A_2} is given by

$$P_{J_{A_2}}^{I_{A_2}} = \sum_{k=1}^{\infty}(q_1)^k(q_2)^{k-1}p_3 = p_3\sum_{k=1}^{\infty}(q_1)^k(q_2)^{k-1}$$

$$= \frac{\mu_2}{\gamma_{A_2}+\mu_2}\frac{\rho_2}{\rho_2+\mu_2}\frac{(\rho_2+\mu_2)(\bar{\gamma}_{A_2})}{\mu_2(\rho_2+\bar{\gamma}_{A_2})} = \frac{\rho_2}{\rho_2+\bar{\gamma}_{A_2}}. \tag{B.16}$$